Symmetry analysis of crystalline spin textures in dipolar spinor condensates

R. W. Cherng and E. Demler

Symmetry analysis of crystalline spin textures in dipolar spinor condensates

R. W. Cherng[1] and E. Demler[1]

[1]Physics Department, Harvard University, Cambridge, MA 02138

We study periodic crystalline spin textures in spinor condensates with dipolar interactions via a systematic symmetry analysis of the low-energy effective theory. By considering symmetry operations which combine real and spin space operations, we classify symmetry groups consistent with non-trivial experimental and theoretical constraints. Minimizing the energy within each symmetry class allows us to explore possible ground states.

I. INTRODUCTION

Experiments in ultracold atomic gases have provided direct and striking evidence for the theory of Bose-Einstein condensation. Typically, the combination of low temperatures and strong magnetic fields freezes out the internal level structure leaving only the density and phase as relevant degrees of freedom. However, recent experimental advancements for multicomponent condensates include optical dipole traps used for preparation [1] and phase-contrast imaging used for detection [2] in $S = 1$ ^{87}Rb.

The magnetization, a vector quantity sensitive to both populations and coherences between hyperfine levels, can be directly imaged in these systems. This has allowed the Berkeley group to observe evidence for spontaneous formation of crystalline magnetic order [3, 4]. When an initially incoherent gas is cooled below the critical temperature, a crystalline lattice of spin domains emerges spontaneously at sufficiently long times.

Several theoretical studies have stressed the role of the effective dipolar interactions [5–8] strongly modified by magnetic field induced rapid Larmor precession and reduced dimensionality [9–11]. This can drive dynamical instabilities in a uniform condensate with characteristic unstable modes at wavevectors in a pattern consistent with observed magnetization correlations [9, 10]. Numerical simulation of the full multicomponent mean-field dynamics also suggests long-lived spin textures [10, 11].

In this paper, we take an alternative approach and focus directly on the low-energy degrees of freedom. In a companion paper [12], we derived a non-linear sigma model describing the dynamics of the magnetization. Due to coupling of the magnetization and superfluid velocity, this effective theory includes a long ranged interaction between skyrmions, topological objects familiar from the theory of ferromagnets [13]. For spinor condensates however, non-zero skyrmion density is directly associated with persistent, circulating superfluid currents.

Our approach to the daunting task of exploring the space of possible ground states is via a systematic symmetry analysis which breaks up this space into distinct symmetry classes. Each of these classes is characterized by invariance under a symmetry group containing combined real space and spin space operations. Litvin and Opechowski called these groups the spin groups [14], a notation we will also use throughout this paper [22]. The
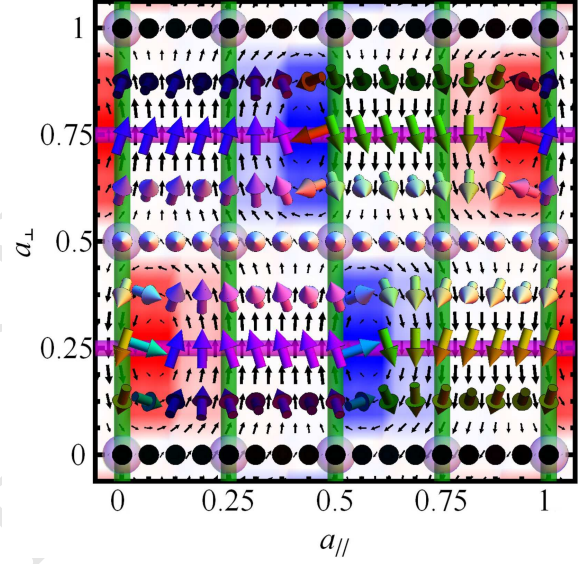

FIG. 1: (Color online) Unit cell for the minimal energy crystalline spin texture. Axis are in units of the lattice constants $a_\parallel = 90$ μm, $a_\perp = 42$ μm. Green vertical lines indicating glide reflection lines, purple horizontal lines indicating mirror lines, and white spheres indicating rotation centers describe symmetry operations. See Fig. 2 for a depiction of symmetry operations. Red background (light grey, center of figure) indicates positive skyrmion density q while blue background (dark grey, left and right edges) indicates negative q. Black 2D arrows indicate the superfluid velocity $\mathbf{v}$, and shaded 3D arrows the magnetization $\hat{n}$. The magnetic field $\hat{B} = \hat{x}$ inducing Larmor precession lies along the horizontal axis in the plane in real space. In spin space, white (black) 3D arrows point along $+\hat{B}$ $(-\hat{B})$.

focus of their paper on the study of magnetically ordered crystals. In such systems, the spin degrees of freedom are localized at discrete atoms. For spinor condensates, the spin-dependent contact interaction which determines the spin healing length is larger than the dipolar interaction strength which determines the size of individual spin domains. Thus we are primarily interested in smooth spin textures and will use spin groups in a novel manner to classify them into distinct symmetry classes.

The power of using spin groups becomes apparent when we consider the non-trivial constraints that spin

textures must satisfy. Theoretical constraints such as a non-vanishing magnetization must be satisfied in order for the low-energy effective theory to be valid. In addition, there are constraints coming from experimental observations such as a vanishing net magnetization. Only a relatively small number of spin groups are compatible with all of these theoretical and experimental constaints and identifying them allows us to significantly narrow the space of possible spin textures.

After identifying the allowed symmetry classes, we then minimize the energy for spin textures within class. This allows us to obtain crystalline spin textures as in Fig. 1 which we find to have the lowest energy for current experimental parameters. These numerical solutions including dipolar interactions are qualitatively similar to the complementary analytical solutions studied in the companion paper [12]. These latter solutions in the absence of dipolar interactions describe periodic configurations of topological objects called skyrmions. The combined results provide a consistent physical picture of the role of dipolar interactions in stabilizing non-trivial crystalline spin textures. In particular, such spin textures can be viewed as a lattice of smooth topological objects carrying persistent superfluid currents.

II. HAMILTONIAN

Here we briefly review the non-linear sigma model describing dipolar spinor condensates derived in the companion paper [12]. We consider $S = 1$ dipolar spinor condensates in a quasi-two-dimensional geometry. Below the scale of spin-independent and spin-dependent contact interactions, the local density is fixed and the magnetization is maximally polarized. Competition between the quadratic Zeeman shift and dipolar interactions determines the formation of spin textures. The following non-linear sigma model describes the effective theory

$$\mathcal{L} = \rho_{2D}\left[-\int dt d^2x \mathcal{A}(\hat{n})\cdot\partial_t\hat{n} - \int dt \mathcal{H}_{KE} - \int dt \mathcal{H}_S\right]$$

$$\mathcal{H}_{KE} = \frac{1}{4m}\int d^2x(\nabla\hat{n})^2 + \frac{1}{2m}\int d^2x d^2y q(x)G(x-y)q(y)$$

$$\mathcal{H}_S = \int d^2x d^2y \hat{n}^i(x)h^{ij}(x-y)\hat{n}^j(y) \tag{1}$$

where the magnetization $\hat{n}$ is a three component real unit vector, $\mathcal{A}(\hat{n})$ is the unit monopole vector potential, $\mathcal{H}_{KE}$ gives kinetic energy contributions, $\mathcal{H}_S$ gives spin-dependent interactions, and ρ_{2D} is the two-dimensional density.

The first term in $\mathcal{H}_{KE}$ is the spin stiffness while the second term comes form the superfluid kinetic energy. Non-uniform textures in $\hat{n}$ arise in part due to phase gradients of the underlying condensate wavefunction. The resulting coupling of $\hat{n}$ to the superfluid velocity $\mathbf{v}$ fixes the vorticity $\epsilon_{\mu\nu}\nabla_\mu\mathbf{v}_\nu = q$ to the skyrmion density

$$q = \epsilon_{\mu\nu}\hat{n}\cdot\nabla_\mu\hat{n}\times\nabla_\nu\hat{n} \tag{2}$$

whose integral is a quantized topological invariant. The superfluid kinetic energy becomes a logarithmic $G(x-y)$ vortex interaction for q where $-\nabla^2 G(x-y) = \delta(x-y)$. Physically, gapless superfluid phase fluctuations generate the long-wavelength divergence of $G(x-y)$.

For $\mathcal{H}_S$, the momentum space interaction tensor is [9]

$$h^{ij}(k) = \tilde{Q}\left(\delta^{ij} + \hat{B}^i\hat{B}^j\right) - \tilde{g}_d\left[\frac{3h(kd_n)-1}{2}\right]\left[\delta^{ij} - 3\hat{B}^i\hat{B}^j\right],$$

$$h(\vec{k}) = [\hat{B}\cdot\hat{k}]^2 w(k) + [\hat{B}\cdot\hat{n}]^2[1-w(k)],$$

$$w(x) = 2x\int_0^\infty dz e^{-(z^2+2zx)} \tag{3}$$

where $\hat{B}$ is a unit vector along the magnetic field, d_n is the thickness of the condensate along the normal direction which we assume to have a Gaussian form, $\tilde{Q} = Q/2$ with Q the quadratic Zeeman shift, $\tilde{g}_d = 4\pi g_d n_{3D}C/3$ with g_d the dipolar interaction stength, n_{3D} the peak three-dimensional density, and $C = 1/\sqrt{2}$ is determined by normalization. For current experimenets [3, 4], $g_d n_{3D} = 0.8$ Hz, $Q = 1.5$ Hz, and $\hat{B}$ is in the plane. For large quadratic Zeeman shifts, all atoms go into the $m_z = 0$ state. This limits our analysis to the small q regime.

III. SPIN TEXTURE CONSTRAINTS

Minimizing the above Hamiltonian is difficult due to a number of non-trivial constraints on possible spin textures. We first consider *fundamental constraints* coming from theoretical considerations for a valid low-energy effective theory.

The first is given by (a) zero net skyrmion charge $\int d^2x q = 0$. This arises due to the long-wavelength divergence of the skyrmion interaction. Recall the skyrmion density acts as a source for superfluid vorticity. The logarithmic interaction between vortices in two dimensions implies that only net neutral configurations of skyrmions have finite energy.

The second is given by (b) maximally polarized magnetization $|\hat{n}| = 1$. Recall the non-linear sigma model derived in the companion paper [12] is valid in the regime where the spin-dependent contact interaction is larger than the dipolar interaction and quadratic Zeeman shift. In this regime, the spin-dependent contact interaction favors a local magnetization that is maximally polarized while the dipolar and Zeeman terms determine the local orientation of the spin texture.

The third is given by (c) explicit symmetry breaking of spin rotational invariance by $\hat{B}$ and the dipolar interaction. In the absence of the dipolar interaction and applied magnetic field, the system is invariant under independent spin-space and real-space rotations/refelctions. The external field along $\hat{B}$ explicitly breaks the spin space symmetry down to rotations/reflections that fix $\hat{B}$ in spin space. For the bare dipolar interaction, the spin-orbit coupling implies that only combined spin-space and real-space rotations remain a symmetry. However, the effec-

tive dipolar interaction is averaged by rapid Larmor precession about the axis of the applied magnetic field $\hat{B}$. The combined effect of the effective dipolar interaction and external field $\hat{B}$ is that independent and arbitrary real-space rotations and spin-space rotations are explicitly broken down to independent real-space rotations and spin-space rotations that fix $\hat{B}$.

Next we consider *phenomenological constraints* coming from properties of the Berkeley group's experimentally observed spin textures. We focus on the spin textures prepared by cooling from the incoherent high-temperature equilibrium state with each hyperfine level having equal initial populations [4].

The fourth constraint is given by (d) periodic crystalline order with a rectangular lattice. Direct real-space imaging of the spin textures shows evidence for a lattice of spin domains. The resulting spin correlation function shows strong peaks in a characteristic cross-like pattern suggestive of a rectangular unit cell.

The fifth is (e) spin textures are not easy axis nor easy plane but cover spin space. All three components of the magnetization can be imaged within the same sample and shows evidence that the spin texture is not confined to vary only along a single axis or a single plane.

The sixth and final is (f) zero net magnetization $\int d^2x \hat{n} = 0$. The distribution of the magnetization vector shows modulations are centered about zero and yield no net magnetization. We note that the Berkeley group has considered spin textures prepared from a non-equilibrium state with imbalanced initial populations. The resulting spin textures carry a net magnetization. Although we do not consider such spin textures directly, they can be studied within the same symmetry analysis framework we describe below.

IV. SPACE GROUPS AND SPIN GROUPS

Having considered the spin texture constraints, we now describe the structure of space groups and their generalization to spin groups in two dimensions. Originally developed in crystallography, we will use them to study smooth spin textures. In particular, we will show in the next section that there are only a small number of compatible spin groups consistent with the above constraints. For a brief overview of group theory and representation theory, see Appendix A.

Crystals of featureless atoms with no internal degrees of freedom can be classified by space groups. For more details on space groups, see Ref. [15, 16]. It is instructive to consider space groups as subgroups of $E(2)$, the two-dimensional Euclidean group of real-space translations and rotations/reflections. We first describe the elements of $E(2)$. The real-space translations are given by a two-component vector t while the rotations/reflections are given by a two-by-two orthogonal matrix M. The resulting group element (M, t) acts on a two-component

position x as

$$x_\mu \to M_{\mu\nu} x_\nu + t_\mu \tag{4}$$

which shows that the product of two elements in $E(2)$ is given by

$$(M', t')(M, t) = (M'M, M't + t') \tag{5}$$

and notice that the real-space rotation has a non-trivial action on the real-space translation. Crystals do not have continuous translation and continuous rotation symmetries of $E(2)$. They describe spontaneous breaking of $E(2)$ down to a discrete set of translations and rotations/reflections called a space group.

First consider groups formed from discrete translations. This forms the Bravais lattice and can be written in terms of the generators t_1, t_2 as $t = ct_1 + dt_2$ where c and d are integers and t_1, t_2 are two component vectors. In two dimensions, there are five distinct Bravais lattices: oblique, rectangular, centered, square, and hexagonal.

Next consider groups formed from discrete rotations/reflections. This forms the point group and can be written in terms of the generators r and s for rotations and reflections as $M = r^a s^b$ where a and b are integers and r, s are two-by-two orthogonal matrices. In two dimensions, there are two classes of point groups: cyclic groups C_n of $2\pi/n$ rotations and dihedral groups D_n of $2\pi/n$ rotations and reflections. For C_n the generators satisfy $r^n = s = \mathbf{1}$ while for D_n the generators satisfy $r^n = s^2 = (rs)^2 = \mathbf{1}$ where $\mathbf{1}$ is the identity element. The order n of C_n and D_n are restricted to $n = 1, 2, 3, 4, 6$. A more detailed discussion of point groups in two dimensions is given in Appendix B.

Notice the Bravais lattice and the point group contain only pure translations and pure rotations/reflections, respectively. Since rotations/reflections can act non-trivially on translations, a space group specifies additional information on how to combine the Bravais lattice and point group. Formally, the Bravais lattice T is a normal subgroup of the space group SG and the proint group PG is the quotient group $PG = SG/T$. In particular, the space group itself can contain non-trivial combinations of translation and rotation/reflection operations. When this is the case, the space group is called non-symmorphic, otherwise it is symmorphic. Viewing the generators t_1, t_2 of the Bravias lattice as elements T_1, T_2 of the space group we can write

$$T_1 = (\mathbf{1}, t_1), \qquad T_2 = (\mathbf{1}, t_2) \tag{6}$$

where t_i is a two-component vector and $\mathbf{1}$ is the 2×2 identity matrix. Viewing the generators of r, s of the point group as elements R, S of the space group we can write

$$R = \left(s(\theta_R), n_1^R t_1 + n_2^R t_2\right), \quad S = \left(r(\theta_S), n_1^S t_1 + n_2^S t_2\right) \tag{7}$$

where the 2×2 rotation and reflection matrices are given by

$$r(\theta_R) = \begin{bmatrix} \cos(\theta) & -\sin(\theta) \\ \sin(\theta) & \cos(\theta) \end{bmatrix},$$

$$s(\theta_S) = \begin{bmatrix} -\cos(2\theta) & -\sin(2\theta) \\ -\sin(2\theta) & \cos(2\theta) \end{bmatrix} \qquad (8)$$

respectively. Then the most general element of the space group is written as

$$(M, t) = R^a S^b T_1^c T_2^d \qquad (9)$$

where a,b,c,d are integers. There are 17 distinct space groups and the corresponding parameters are adapted from Ref. [17] and given in Table I.

Litvin and Opechowski [14] considered the classification of magnetically ordered crystals of atoms with internal spin degrees of freedom via spin groups. These groups are generalizations of space groups with combined real space translations, real-space rotations/reflections, as well as spin-space rotations/reflections. Here we consider how they can be explicitly constructed from the representation theory of space groups more suitable for calculations. Litvin and Opechowski consider a more implicit classification of spin groups which we show is equivalent in Appendix C.

It is instructive to consider spin groups as subgroups of the direct product $E(2) \otimes O(3)$, where $E(2)$ is the two-dimensional Euclidean group of real-space translations and rotations/reflections and $O(3)$ is the three-dimensional orthogonal group of spin-space rotations/reflections. Recall the real-space translations are given by a two-component vector t while the rotations/reflections are given by a two-by-two orthogonal matrix M. In addition the spin-space rotations/reflections are given by a three-by-three orthogonal matrix O. The resulting group element (M, t, O) acts on a three-component spin $\hat{n}(x)$ that is a function of a two-component position x as

$$\hat{n}^i(x_\mu) \rightarrow O^{ij} \hat{n}^j(M_{\mu\nu} x_\nu + t_\mu) \qquad (10)$$

which shows that the product of two elements in $E(2) \otimes O(3)$ is given by

$$(M', t', O')(M, t, O) = (M'M, M't + t', O'O) \qquad (11)$$

and notice that while the real-space rotation has a nontrivial action on the real-space translation, the real-space and spin-space operations do not act on each other. Magnetically ordered crystals do not have continuous real-space translation, real-space rotation, and continuous spin-space rotations symmetries of $E(2) \otimes O(3)$. They describe spontaneous breaking of $E(2) \otimes O(3)$ down to a discrete set of real-space translations, real-space rotations/reflections, and spin-space rotations/reflections called a spin group.

To construct spin groups, start by choosing a space group SG giving the real-space operations. Now choose a three-dimensional orthogonal representation ϕ of the space group SG. This is a function from SG to three-dimensional orthogonal matrices satisfying the homomorphism condition

$$\phi(M', t')\phi(M, t) = \phi(M'M, M't + t') \qquad (12)$$

For this representation ϕ, choose a group of three-dimensional orthogonal matrices N that satisfies

$$\phi(M, t)^{-1} N \phi(M, t) = N \qquad (13)$$

consisting of three-by-three orthogonal matrices that are left fixed under conjugation by $\phi(M, t)$ for all elements (M, t) of the the space group SG. The resulting spin group has elements of the form

$$(M, t, O) = (M, t, n\phi(M, t)) \qquad (14)$$

where (M, t) are the elements of a space group SG, ϕ is a representation of SG, and n is an element of N. The most general space group element is of the form in Eq. 9. Using the space group product of Eq. 9 and homomorphism condition Eq. 12, we see that

$$\phi(R^a S^b T_1^c T_2^d) = \phi(R)^a \phi(S)^b \phi(T_1)^c \phi(T_2)^d \qquad (15)$$

meaning we only need to specify the values of the representation on the space group generators.

V. COMPATIBLE SPIN GROUPS

Before discussing how to impose the constraints of Sec. III, we first discuss the physical interpretation of the structure of spin groups. Recall that a spin group is given by a choice of space group SG with elements (M, t), three-dimensional orthogonal representation ϕ, and a choice of three-dimensional orthogonal matrices N that commute as a set with each $\phi(M, t)$.

First consider the group N. From Eq. 14, we see that by taking $M = \mathbf{1}$ with $\mathbf{1}$ the 2×2 identity matrix and $t = 0$, the spin group contains the elements $(\mathbf{1}, 0, n)$ where n is an element of N. The physical interpretation is that N describes global spin-space symmetries that do not act on spatial degrees of freedom. For example, a uniform magnetization is described by N containing rotations and reflections that leave the magnetization fixed.

Next consider the group given by the kernel $\ker(\phi)$ of the representation. This consists of elements (M', t') that satisfy $\phi(M', t') = \mathbf{1}$ with $\mathbf{1}$ the 3×3 identity matrix. These elements form a space group SG' that is a subgroup of SG. From Eq. 14, we see that the spin group contains the elements $(M', t', \mathbf{1})$. The physical interpretation is that SG' describes global real-space symmetries that do not act on spin degrees of freedom. The distinction between SG and SG' is that SG describes the symmetries of the *crystallographic unit cell* while SG' describes the symmetries of the *magnetic unit cell*.

SG	Type	Lat.	t_1	t_2	PG	θ_R	n_1^R	n_2^R	θ_S	n_1^S	n_2^S
$p1$	sym	Oblique	$(a\cos(\gamma), a\sin(\gamma))$	$(0,b)$	C_1	0	0	0	—	—	—
$p211$	sym	Oblique	$(a\cos(\gamma), a\sin(\gamma))$	$(0,b)$	C_2	π	0	0	—	—	—
$p1m1$	sym	Rectangular	$(a,0)$	$(0,b)$	D_1	0	0	0	0	0	0
$p1g1$	non	Rectangular	$(a,0)$	$(0,b)$	D_1	0	0	0	0	0	$1/2$
$c1m1$	sym	Centered	$(a/2,b/2)$	$(0,b)$	D_1	0	0	0	0	0	0
$p2mm$	sym	Rectangular	$(a,0)$	$(0,b)$	D_2	π	0	0	0	0	0
$p2mg$	non	Rectangular	$(a,0)$	$(0,b)$	D_2	π	0	0	0	$1/2$	0
$p2gg$	non	Rectangular	$(a,0)$	$(0,b)$	D_2	π	0	0	0	$1/2$	$1/2$
$c2mm$	sym	Centered	$(a/2,b/2)$	$(0,b)$	D_2	π	0	0	0	0	0
$p4$	sym	Square	$(a,0)$	$(0,a)$	C_4	$\pi/2$	0	0	—	—	—
$p4mm$	sym	Square	$(a,0)$	$(0,a)$	D_4	$\pi/2$	0	0	0	0	0
$p4gm$	non	Square	$(a,0)$	$(0,a)$	D_4	$\pi/2$	0	0	0	$1/2$	$1/2$
$p3$	sym	Hexagonal	$(a\sqrt{3}/2, -a/2)$	$(0,a)$	C_3	$2\pi/3$	0	0	—	—	—
$p3m1$	sym	Hexagonal	$(a\sqrt{3}/2, -a/2)$	$(0,a)$	D_3	$2\pi/3$	0	0	$-\pi/6$	0	0
$p31m$	sym	Hexagonal	$(a\sqrt{3}/2, -a/2)$	$(0,a)$	D_3	$2\pi/3$	0	0	0	0	0
$p6$	sym	Hexagonal	$(a\sqrt{3}/2, -a/2)$	$(0,a)$	C_6	$\pi/3$	0	0	—	—	—
$p6mm$	sym	Hexagonal	$(a\sqrt{3}/2, -a/2)$	$(0,a)$	D_6	$\pi/3$	0	0	$-\pi/6$	0	0

TABLE I: The seventeen two-dimensional space groups (SG) have elements of the form $(M,t) = R^a S^b T_1^c T_2^d$. Here a, b, c, d are integers. Each space group is one of two types (Type) symmorphic (sym.) or non-symmorphic (non). The normal subgroup of translations T is one of four Bravais lattice types (Lat.) with the generators T_1, T_2. The quotient group SG/T is the point group (PG) and has generators R, S. The parameters t_1, t_2 specify the generators T_1, T_2 through Eq. 6. The parameters $\theta_{R,S}$, $\theta_{R,S}$, $n_{1,2}^{R,S}$ specify the generators R, S through Eqs. 7, 8. Adapted from Ref. [17].

Consider a square lattice with lattice constant a and one spinful atom per unit cell and anti-ferromagnetic order. The crystallographic unit cell is generated by the vectors $(0,a)$ and $(a,0)$ and contains one spinful atom. This is the unit cell ignoring spin and described by a space group SG. The magnetic unit cell is generated by the vectors $(+a,-a)$ and $(-a,+a)$ and contains two spinful atoms. This is the unit cell taking into account spin and described by a space group SG' that is a subgroup of SG.

From now on, we focus on applications of spin groups to classify smooth spin textures. In order to understand which spin groups are compatible with the constraints discussed earlier, we consider how these symmetry operations act on the magnetization vector $\hat{n}$ and skyrmion density q. In real space, an element (M,t,O) of a spin group acts as

$$\hat{n}^i(x_\mu) \to O^{ij}\hat{n}^j(M_{\mu\nu}x_\nu + t_\mu),$$
$$q(x_\mu) \to \det[O]\det[M]q(M_{\mu\nu}x_\nu + t_\mu) \quad (16)$$

where we have used Eq. 10 for the action on $\hat{n}$ which along with Eq. 2 allows us to deduce the action on q. In momentum space, the action is

$$\hat{n}^i(k_\mu) \to \exp(ik_\mu M_{\mu\nu}^{-1}t_\nu)O^{ij}\hat{n}^j(M_{\mu\nu}k_\nu),$$
$$q(k_\mu) \to \exp(ik_\mu M_{\mu\nu}^{-1}t_\nu)\det[O]\det[M]q(M_{\mu\nu}k_\nu) \quad (17)$$

which follow directly from the Fourier transform.

It is also helpful to visualize the action of the group elements on spin textures and their corresponding skyrmion

densities. For example, in Fig. 2a, we show the action of a real-space reflection about the thick horizontal purple mirror line combined with spin-space reflection $\hat{n}_\parallel \to -\hat{n}_\parallel$ of the component along $\hat{B}$. The spin texture in the back panel which is entirely below the purple horizontal line is mapped to be above the purple horizontal line in the front panel. In addition, the spins that point along $-\hat{B}$ below the purple horizontal line to point along $+\hat{B}$ above the purple horizontal line. Since spins on the purple horizontal line are mapped to themselves, consistency with the action Eq. 16 implies the $\hat{B}$ component in spin-space must vanish. This ensure continutiy of the spin texture across the purple line. For pure reflections about one axis, the corresponding determinant of the real space reflection $\det[O]$ is negative. In addition, the determinant of the matrix describing the spin space reflection $\hat{n}_\parallel \to -\hat{n}_\parallel$ is also negative. Since the skyrmion density transforms with the product of the determinants, it has the same sign going from below the thick purple horizontal line in the back panel to above it in the front panel.

In addition to reflection about mirror lines, we also show translations followed by reflections about glide mirror lines combined with full spin-space inversion in Fig. 2b. The corresponding spin group operations shows a non-trivial combination of all three real-space translation, real-space reflection, and spin-space inversion. Notice it leaves no point in real-space fixed Fig. 2c shows a real-space rotation combined with inversion of the component perpendicular to $\hat{B}$ in spin-space. It leaves the
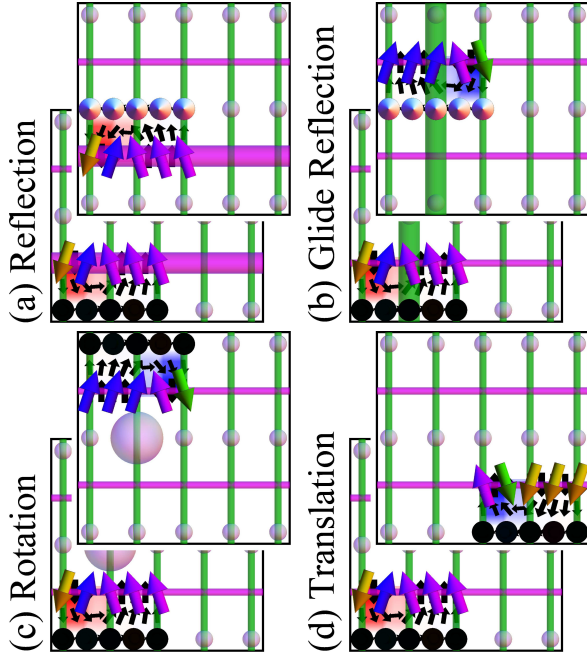
FIG. 2: (Color online) Figures **a-d** illustrates spin group operations that combine non-trivial spin-space and real-space actions. One element of the spin group acts as a real-space reflection about the thick purple horizontal mirror line combined with spin-space reflection $\hat{n}_\parallel \to -\hat{n}_\parallel$ of the component along $\hat{B}$. Recall 3D arrows indicate the magnetization $\hat{n}$ with white (black) 3D arrows pointing along $+\hat{B}$ ($-\hat{B}$). This action of this operation on the back panel is shown in the front panel of **(a)**. Notice spins pointing along $-\hat{B}$ below the thick purple line map to those along $+\hat{B}$ above. Those on the thick horizontal purple are mapped to themselves and are perpendicular to $\hat{B}$ in spin space. **(b)** shows a vertical translation followed by reflection along a glide mirror line (thick green vertical line) combined with $\hat{n}_{\perp,1} \to -\hat{n}_{\perp,1}$, $\hat{n}_\parallel \to -\hat{n}_\parallel$ **(c)** π-rotation about a rotation center (large white sphere) combined with $\hat{n}_{\perp,1} \to -\hat{n}_{\perp,1}$, **(d)** horizontal translation combined with $\hat{n}_{\perp,1} \to -\hat{n}_{\perp,2}$ where $\hat{n}_{\perp,1}$, $\hat{n}_{\perp,2}$ are the two components perpendicular to $\hat{B}$.

rotation point fixed with the spin along $+\hat{B}$. Finally, we show a translation combined with spin-space reflection in Fig. 2d.

We now begin the analysis of the constraints in Section III. Recall that a spin group is given by a choice of space group SG with elements (M, t), three-dimensional orthogonal representation ϕ, and a choice of a group of three-dimensional orthogonal matrices N that satisfy $\phi(M, t)^{-1} N \phi(M, t) = N$.

We first use the constraints to identify the space group SG. To do this, we need to specify the Bravais lattice and point group. The constraint (d) states that the observed spin textures directly identify the Bravais lattice as rectangular. From constraint (c), real-space rotation/reflection symmetry is explicitly broken to the dihedral group D_2 that leaves the magnetic field $\hat{B}$ fixed.

In general, we do not expect the spin texture to have a higher symmetry than the Hamiltonian itself which suggests the point group symmetry should not be larger than D_2. In principal, the point group symmetry could be spontaneously broken to a smaller point group. However, we assume this does not occur and take the point group to be D_2. Referring to Table I, we see there are a total of three space groups with a rectangular Bravais lattice and D_2 point group: $p2mm$, $p2mg$, $p2gg$.

Now we turn to identifying the group N. Recall N has the physical interpretation of describing the global spin-space symmetries that do not act on spatial degrees of freedom. In particular, if there is a non-trivial rotation in N, the spin texture then must lie along that axis. If there is a non-trivial reflection, the spin texture must lie in the plane fixed by the reflection. Constraint (e) states that spin textures cover spin space and are not confined to a single axis or plane. This implies that N must be the trivial group and there are no global spin-space symmetries.

Finally, we turn to the identification of the representation ϕ. The basic principle is to first enumerate all off the three-dimensional orthogonal representations for the space groups $p2mm$, $p2mg$, $p2gg$. We use techniques described in [15, 16] in order to study two-dimensional complex unitary representations and anti-unitary co-representations to then analyze the needed three-dimensional real orthogonal representations. Enumeration of these representations is the most mathematically involved part of the analysis and is discussed in detail in the following appendices. Appendix A contains a discussion of of unitary representations, anti-unitary co-representations, and orthogonal representations as well as how to construct them. Appendix B collects detailed information about point groups in two dimensions necessary for the construction of space group representations. Appendix D applies the results of the above two appendices to the construction of unitary representations and anti-unitary co-representations of space groups. Appendix E presents a illustrative example explicitly constructing the spin group for the minimal energy spin texture shown in Fig. 1. Finally, Appendix F discusses how the compatible spin groups in Table II are selected from the enumeration of all possible spin groups in more detail. We give a brief overview of this process below.

After enumerating all of the representations and obtaining the associated spin groups, we study the real-space and momentum-space actions on both the magnetization $\hat{n}$ and skyrmion density q in Eqs. 16 and 17.

For a point x, consider spin group operations (M, t, O) that leave x fixed. The magnetization vector $\hat{n}$ must then be left fixed by all of the associated spin-space operations O. From constraint (b), there must be a non-trivial subspace left fixed by O because otherwise the magnetization vector would vanish at x. In momentum space, consider the wavevector $k = 0$. Similar considerations show that for the spin group operations (M, t, O) that leave $k = 0$ fixed, the spin-space operations O must leave the net

SG	BWSG	SG$^{1/2}$	k	PG$_k$	ψ^{PG_k}	$\phi(T_1)$	$\phi(T_2)$	$\phi(R)$	$\phi(S)$	a	b	E
p2mm	p(2a)2m'm'	p2mg	$(\pi/a_1,0)$	D$_2$	E$_1$	$--\hat{-}$	$++\hat{+}$	$-+\hat{-}$	$++\hat{-}$	9	**7**	-0.49
p2mm	p(2a)2mm	p2mm	$(\pi/a_1,0)$	D$_2$	A$_0$,B$_1$	$\hat{-}--$	$\hat{+}++$	$\hat{-}-+$	$\hat{-}-+$	5	**9**	-0.52
p2mg	—	—	$(\pi/a_1,0)$	D$_2$	E$_1$	$+\hat{+}+$	$+\hat{+}+$	$-\hat{+}-$	$-\hat{-}+$	5	**9**	-0.88
p2mg	p2'm'g'	p1m1	$(\pi/a_1,0)$	D$_1$	A$_0$,A$_1$	$++\hat{+}$	$++\hat{+}$	$++\hat{-}$	$--\hat{+}$	7	**9**	-0.26
p2mg	p(2b)2m'g'	p2gg	$(\pi/a_1,0)$	D$_2$	E$_1$	$+\hat{+}+$	$-\hat{+}+$	$-\hat{+}-$	$+\hat{-}+$	4.2	**4.5**	-0.99
p2mg	p(2b)2m'g'	p2gg	$(0,\pi/a_2)$	D$_2$	E$_1$	$\hat{+}++$	$\hat{-}--$	$\hat{-}+-$	$\hat{+}+-$	**9**	7	-0.76
p2mg	p(2b)2m'g'	p2gg	$(\pi/a_1,\pi/a_2)$	D$_2$	E$_1$	$+\hat{+}+$	$-\hat{-}-$	$-\hat{-}+$	$+\hat{+}-$	**7**	9	-0.71
p2mg	p(2b)2mg	p2mg	$(\pi/a_1,0)$	D$_2$	E$_1$	$++\hat{+}$	$-+\hat{+}$	$-+\hat{-}$	$--\hat{+}$	9	**9**	-0.25
p2mg	p(2b)2mg	p2mg	$(0,\pi/a_2)$	D$_2$	E$_1$	$\hat{+}++$	$\hat{-}--$	$\hat{-}-+$	$\hat{+}++$	**9**	3	-0.76
p2gg	—	—	$(\pi/a_1,0)$	D$_2$	E$_1$	$\hat{+}++$	$\hat{+}++$	$\hat{-}+-$	$\hat{-}-+$	**3**	4	-0.89
p2gg	p2'gg'	p1g1	$(\pi/a_1,0)$	D$_1$	A$_0$,A$_1$	$++\hat{+}$	$++\hat{+}$	$++\hat{-}$	$--\hat{+}$	5	**5**	-0.85

TABLE II:

Table of spin space operations associated with the generators of real space operations for compatible spin groups consistent with all constraints. For each space group SG describing real space operations generated by translations T_1, T_2, rotations R, and refelctions S, there are multiple ways to associate a real orthogonal representation of SG that defines the combined spin-space operations $\phi(T_1)$, $\phi(T_2)$, $\phi(R)$, $\phi(S)$. Signs indicate the diagonal entries of the corresponding matrix acting in spin-space.

Each of these real orthogonal representations is built from either a unitary representation of SG or anti-unitary representation or a black-white space group $BWSG$ with halving subgroup $SG^{1/2}$. The corresponding unitary representations and anti-unitary co-representations are specified by the wavevector k, wavevector point group PG_k, and projective representation ψ^{PG_k}. For more details, see Appendices D, E, and F.

Minimal energy crystalline spin textures for each resulting symmetry group have lattice constants a, b in units of 10 μm for the translations T_1, T_2 and energy E scaled by $g_d n_{3D}$ where g_d is the dipolar interaction strength and n_{3D} is the peak three-dimensional density. For ϕ, the bold entry with a hat indicates the component parallel to $\hat{B}$. For real space lattice constants a, the bold italic entry indicates the component parallel to $\hat{B}$.

magnetization $\hat{n}(k=0)$ fixed. Unlike in real space, constraint (f) implies there is no subspace left fixed by O in order to have vanishing net magnetization. Constraint (a) implies that at least one of the (M,t,O) that leave $k=0$ fixed, must have $\det[0]\det[M]=-1$ in order to have vanishing net skyrmion charge.

There are only 11 orthogonal representations and thus spin groups that satisfy all of the above constraints arising from the real-space and momentum space actions. The most general element of the spin group is given by Eq. 14. Since n is always the identity element because N is the trivial group, we need $\phi(M,t)$ for a general element (M,t) of the corresponding space group. From Eq. 15, we see that we only need to specify the values of the representation for the generators R, S for rotation, reflections and T_1, T_2 for translations. Table II gives these values for all of the compatible spin groups. In addition, we also list the corresponding values of the optimized lattice constants and energies obtained in the numerical analysis of the next section.

VI. MINIMAL ENERGY SPIN TEXTURES

Identifying the compatible spin groups allows us to divide the space of possible spin textures into symmetry classes. In this section, we describe the numerical optimization used to obtain minimal energy spin textures.

We consider the spin texture

$$\hat{n}(u_1, u_2) = \hat{n}(u_1 t_1/N_1 + u_2 t_2/N_2) \tag{18}$$

where we take the spin texture to be in the symmetry class described by a spin group with basis vectors t_1 and t_2. Next we impose the spin group symmetry operations given by 16. By using the lattice of real-space translations, we restrict our attention to the unit cell with $0 \leq u_i < N_i$. This corresponds to $N_1 \times N_2$ discretized points for the spin texture.

However, the number of independent points within each unit cell is smaller due to the presence of point group operations. For each point $x = u_1 t_1/N_1 + u_2 t_2/N_2$, consider the space group elements (M,t) that fix x. The associated $\phi(M,t)$ in the spin group must leave $\hat{n}(x)$ invariant and gives the space of allowed $\hat{n}$ at the point x. In addition, for (M,t) that takes x to a different point x', the magnetization at the latter point is given solely in terms of the magnetization at the former through $\hat{n}(x) = \hat{n}'(x') = \phi(M,t)\hat{n}(Mx+t)$ in a notation with suppressed indices. The independent points are given by $0 \leq u_i \leq N_i/N_i'$ with N_i/N_i' an integer. For the compatible spin groups in Table II we have $N_i/N_i' = 2$.

This smaller region of $N_1' \times N_2'$ points contained within the unit cell of $N_1 \times N_2$ points is called the fundamental region. By specifying the spin texture within the fundamental region, we can construct the entire spin texture via the spin group operations. The action of the point group operations along with their associated spin-space

actions determine the spin texture within the unit cell given its values in the fundamental region. In particular, each element of the point group maps the fundamental region into a distinct region within the unit cell. This gives the ratio of the number of points in the fundamental region to the number of points in the unit cell as the order or number of group elements for the point group. For the compatible spin groups, the point group is D_2 which is of order 4.

The action of the translation operations along with their associated spin-space actions determine the spin texture for different unit cells. This is shown in Fig. 2 where the spin texture for coordinates in the lower left corner specifies the entire spin texture for all coordinates through the symmetry group operations.

Finally, we turn to energy minimization of the resulting symmetry adapted discretization. The non-local skyrmion and dipolar interactions provides the main difficulty which we handle via Ewald summation [18]. We separate each of these interactions into short-ranged and long-ranged contributions calculate their contributions in real and momentum space, respectively. In order to approximate smooth spin textures, it is useful to perform an interpolation step on the discretized values before calculating the energy. Since the magnetization $\hat{n}$ is a unit vector living on the sphere, this becomes a problem of spherical interpolation which we address in detail in Appendix G.

For each compatible spin group, we use an 8×8 discretization, fix the lattice constants a, b and minimize the energy E with respect to the discretized spin texture $\hat{n}(x)$. We then minimize with respect to the lattice constants a, b. The results are shown in Table II for a, b in units of 10 μm and E scaled by the dipolar interaction energy $g_d n_{3D}$. We check for convergence by repeating the above procedure for a 16×16 discretization for a_1, a_2 near the previously optimized values.

A more refined optimization of a, b gives the additional significant figures for the minimal energy crystalline spin texture. The unit cell for this spin texture showing the magnetization $\hat{n}$, skyrmion density q, and superfluid velocity $\mathbf{v}$ is shown in Fig. 1. From Table II, notice t_1 (t_2) giving translations perpendicular (parallel) to $\hat{B}$ have trivial (non-trivial) spin space operations. This is similar to the distinction between the unit cell and magnetic unit cell for magnetically ordered crystals. Fig. 1 plots the analog of the magnetic unit cell. Pure real-space translations without any spin-space operations are sufficient to generate the rest of the spin texture. In contrast, the unit cell corresponds to only the left (equivalently right) half of the magnetic unit cell. These halves are related by a spin group operation combining a real-space translation and non-trivial spin-space operation.

This means that the magnetic unit cell lattice constants are related to the spin grip unit cell lattice constants by $a_\parallel = 2b$ ($a_\perp = a$). We also plot the momentum space structure factors for components of the magnetization perpendicular and parallel to $\hat{B}$ in Fig. 3.
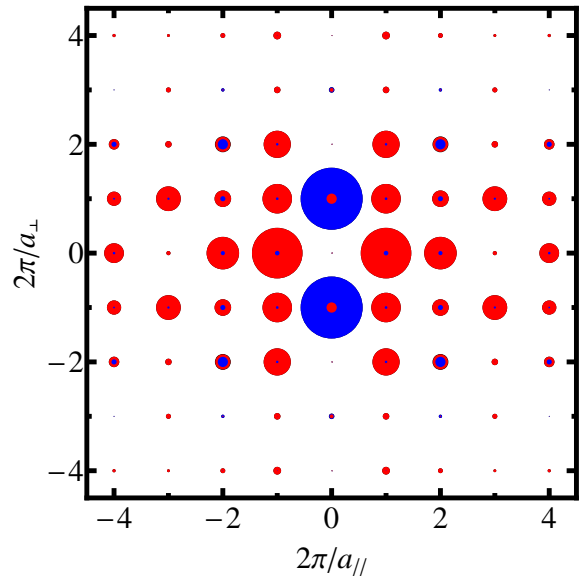

FIG. 3: (Color online) Momentum space structure factor $\hat{n}(k)$ for the minimal energy crystalline spin texture of Fig. 1. The magnetic field $\hat{B}$ is along the horizontal axis while the axis are in units of the inverse wavevector with lattice constants $a_\parallel = 90$ μm, $a_\perp = 42$ μm. The area of dark blue (light red) disks is proportional to the magnitude of components parallel (perpendicular) to $\hat{B}$.

VII. DISCUSSION

With the symmetry analysis and energy minimization completed, we now discuss the structure of the resulting crystalline spin textures. We first focus on the minimal energy spin texture shown in Figs. 1, 3. From the momentum space spin structure factors in Fig. 3, spin components parallel (perpendicular) to $\hat{B}$ have weight concentrated at wavevectors perpendicular (parallel) to $\hat{B}$. This anisotropy in the structure factor weights maximizes the gain in the dipolar interaction energy in Eq. 3. This pattern is also consistent with the characteristic cross-like structure for observed spin structure factors [3, 4]. It also agrees with the pattern of unstable modes obtained from a dynamical instability analysis of the uniform state [9, 10].

Notice that such a spin texture has a non-vanishing skyrmion density q as shown in Fig. 1. This follows from Eq. 2 showing $q \neq 0$ when orthogonal components of $\hat{n}$ vary along orthogonal directions. Since the vorticity of the superfluid velocity $\mathbf{v}$ is given by q, this implies the presence of persistent, circulating superfluid currents.

Consider the components $\hat{n}_\parallel$ ($\hat{n}_\perp$) parallel (perpendicular) to $\hat{B}$ separately in the region $0 \leq x_\parallel \leq a_\parallel/2$, $0 \leq x_\perp \leq a_\perp/2$ of Fig. 1 where $x_\parallel$ ($x_\perp$) are coordinates parallel (perpendicular) to $\hat{B}$. Symmetry operations give the spin texture in all other regions. We can characterize

the behavior of parallel components as $\hat{n}_\parallel \sim \cos(k_\perp x_\perp)$ varying over the entire range ± 1 while perpendicular components $\hat{n}_{\perp,1} + i\hat{n}_{\perp,2} \sim \sqrt{1 - \hat{n}_\parallel^2} \exp(ik_\perp x_\perp)$ have a spiral winding in regions between $\hat{n}_\parallel = \pm 1$. The dipolar interaction favors this configuration and gives rise to a non-vanishing skyrmion density q and superfluid velocity $\mathbf{v}$.

In the companion paper, we showed spin textures of this form arise naturally even in the absence of dipolar interactions as non-trivial analytical solutions of the effective theory with spin stiffness and skymrion interactions. There they have an interpretation as neutral stripe configurations of skyrmions and anti-skyrmions. Turning on dipolar interactions makes such solutions more stable compared to the uniform state.

In conclusion, we have considered the low-energy effective theory for dipolar spinor condensates. The resulting non-linear sigma model describes the dynamics of the magnetization and includes spin stiffness, skyrmion interaction, and dipolar interaction terms. A systematic analysis of symmetry operations containing combined real space and spin space actions allows us to classify the allowed symmetry groups consistent with non-trivial theoretical and experimental constraints on possible spin textures. Possible ground states describing neutral collections of topological skyrmions carrying persistent superfluid currents are obtained by minimizing the energy within each symmetry class.

Appendix A: Group theory and representation theory

To provide background for the analysis of spin groups, we review here aspects of group theory and representation theory. Beginning with general definitions for group and representations, we then discuss unitary representations of groups and their generalization to projective unitary representations. Then we consider how projective unitary representations are used in the construction of the unitary representations of a group with a normal abelian subgroup. Next we present anti-unitary co-representations and how to construct them from the unitary representations of a halving subgroup. Finally, we analyze the real orthogonal representations relevant for spin groups and how to obtain them from unitary representations and anti-unitary co-representations. For more details on group theory, see Ref. [19]. For applications of group theory to the study of space groups, see Refs. [15, 16].

1. Group theory

A group G is a set of elements g with a binary operation $G \times G \to G$ usually called multiplication satisfying the axioms of closure $g_1 g_2 \in G$, associativity $(g_1 g_2)g_3 = g_1(g_2 g_3)$, identity $\mathbf{1}g = g$ for the identity element $\mathbf{1}$, and inverse $g^{-1}g = \mathbf{1}$ for the inverse element g^{-1}. $|G|$ is the order or number of elements in the group.

A subgroup H of a group G is a subset of elements h in G that also form a group under multiplication in G. A normal subgroup N of a group G is a subgroup that is left fixed by conjugation $g^{-1}Ng = N$ for all elements g in G. An abelian group is a group that is commutative $g_1 g_2 = g_2 g_1$.

When H is a subgroup of G, the equivalence relation $g_1 \sim g_2$ for $g_1^{-1}g_2 \in H$ divides G into distinct equivalence classes. For representatives r_i, the left cosets $r_i H$ form the equivalence classes $G = \cup_i r_i H$. Similarly, the right cosets Hg_i also form the equivalence classes $G = \cup_i Hr_i$. A normal subgroup has the same left and right cosets $r_i H = Hr_i$. In this case, the left (equivalently the right) cosets form a group called the quotient group G/H with multiplication defined by $r_1 r_2 = r_3(r_1, r_2)$ where $r_3(r_1, r_2)$ is defined as the coset representative that satisfies $r_1 r_2 H = r_3(r_2, r_2)H$.

A group homomorphism ϕ from group G to group H is a map $G \to H$ that is compatible with both of the group multiplications. This means that ϕ satisfies the homomorphism condition $\phi(g_1)\phi(g_2) = \phi(g_1 g_2)$. The kernel $\ker(\phi)$ consists of the elements of G that map to the identity element in H, $\phi(g) = \mathbf{1}$. The kernel is a normal subgroup of G. The image $\mathrm{im}(\phi)$ consists of the elements of H that occur for some element g of G. The image is a subgroup of H. A surjective map ϕ is equivalent to $\mathrm{im}(\phi) = G$ being the entire group H. An injective map ϕ is equivalent to $\ker(\phi) = \mathbf{1}$ being the trivial group consisting of the identity element alone. A bijective map ϕ is called an isomorphism.

2. Group representations

A representation ϕ is a homomorphism from a group G to the group of linear transformations on some finite dimensional vector space V. This means that for each group element g in G, $\phi(g) = M$ where M is an invertible matrix. Here ϕ is subject to the homomorphism condition

$$\phi(g_1)\phi(g_2) = \phi(g_1 g_2) \tag{A1}$$

Two representations ϕ, ϕ' are equivalent if there is a fixed matrix S such that

$$S^{-1}\phi(g)S = \phi'(g) \tag{A2}$$

for all group elements g in G. A representation is irreducible if the action of the group through $\phi(g)$ leaves no non-tirival subspace fixed. The primary goal of group representation theory is to classify and construct all of the inequivalent irreducible representations.

3. Unitary representations

A unitary represenation ϕ_U is a homomorphism from a group G to the group of finite-dimensional unitary transformations. This means that for each group element g in G, $\phi_U(g) = U(G)$ is a finite-dimensional complex unitary matrix satisfying

$$U(g)^{-1} = U(g)^\dagger \tag{A3}$$

where $\dagger$ denotes the adjoint or complex conjugate transpose. Here, ϕ_U is subject to the homomorphism condition

$$\phi_U(g_1)\phi_U(g_2) = \phi_U(g_1g_2) \tag{A4}$$

for each element g_1, g_2 in the group G. In particular, this implies

$$U(g_1)U(g_2) = U(g_1g_2) \tag{A5}$$

for the unitary matrices associated to the elements g_1, g_2 in the group G.

4. Projective unitary representations

A projective unitary representation ψ_U is a homomorphism from a group G to the group of finite-dimensional projective unitary transformations. Projective unitary transformations that only differ by multiplication by a complex scalar are considered the same. In constrast, unitary transformations the differ by multiplication by a complex scalar are distinct. This means that for each group element g in G, $\psi_U(g) = U(G)$ is a finite-dimensional complex unitary matrix satisfying

$$U(g)^{-1} = U(g)^\dagger \tag{A6}$$

where $\dagger$ denotes the adjoint or complex conjugate transpose. Here, ψ_U is subject to the projective homomorphism condition

$$\psi_U(g_1)\psi_U(g_2) = \lambda(g_1, g_2)\psi_U(g_1g_2) \tag{A7}$$

where $\lambda(g_1, g_2)$ is the factor system for the projective representation and is a complex scalar for all elements g_1, g_2 in the group G. In particular, this implies

$$U(g_1)U(g_2) = \lambda(g_1, g_2)U(g_1g_2) \tag{A8}$$

for the unitary matrices associated to the elements g_1, g_2 in the group G.

The factor system $\lambda(g_1, g_2)$ is subject to the associativity condition

$$\lambda(g_1, g_2)\lambda(g_1g_2, g_3) = \lambda(g_1, g_2g_3)\lambda(g_1, g_2) \tag{A9}$$

Two projective representations ψ'_U, λ' and ψ_U, λ are projectively equivalent if there exists a fixed matrix S and non-zero complex scalar function $l(g)$ such that

$$S^{-1}\psi_U(g)S/l(g) = \psi'_U(g) \tag{A10}$$

from which we can see that the factor systems are related by

$$\lambda'(g_1, g_2) = \frac{\lambda(g_1, g_2)}{l(g_1)l(g_2)} \tag{A11}$$

Projective equivalence divides the projective representations of a group into equivalence classes. From each equivalence class, we can choose a normalized and standard factor system representative subject to the normalization and standardization conditions

$$|\lambda(g_1, g_2)| = 1, \quad \lambda(g, \mathbf{1}) = \lambda(\mathbf{1}, g) = \lambda(\mathbf{1}, \mathbf{1}) = 1 \tag{A12}$$

where $\mathbf{1}$ is the identity element.

5. Induced and subduced representations

Consider a group G with a subgroup H of index $I = |G|/|H|$ where recall $|G|$ denote the order or number of elements in group G. The left coset decomposition of G by H is given by

$$G = \cup_i r_i H \tag{A13}$$

where $r_1 \ldots r_I$ are left coset representatives. For a $N \times N$ dimensional unitary representation ϕ^H of the subgroup G, the induced representation $\phi^{H\uparrow G}$ of the group G is a $IN \times IN$ dimensional unitary representation

$$\phi^{H\uparrow G}(g)_{ij} = \sum_{h \in H} \phi^H(h)\delta(h, r_i^{-1}gr_j) \tag{A14}$$

where δ is the Kronecker delta function. In the notation above, when $r_i^{-1}gr_j = h$, the i row and j column with $1 \leq i, j \leq I$ of $\phi^G(g)$ consists of the $N \times N$ matrix $\phi^H(h)$.

Given a unitary representation of ϕ^G of G, the subduced representation $\phi^{G\downarrow H}$ is given by

$$\phi^{G\downarrow H}(h) = \phi^G(h) \tag{A15}$$

and is a unitary representation of H which corresponds to restriction to the elements h of H for ϕ^G. The induced representation ϕ^G gives a unitary representation of G from a unitary representation ϕ^H of a subgroup H.

6. Little groups and small representations

Given an irreducible unitary representation ϕ^H of a subgroup H of G, the little group G_{ϕ^H} is the largest subgroup of G that leaves ϕ^H fixed under conjugation. This means that G_{ϕ^H} consists of all elements g in G for which $\phi^H(g^{-1}hg) = \phi^H(h)$ is true for all elements of h in H. From this, it is clear that H is a subgroup of G_{ϕ^H}.

A small representation $\phi^{G_{\phi^H}}$ of the little group G_{ϕ^H} is a unitary representation of G_{ϕ^H} that subduces to ϕ^H

$$\phi^{G_{\phi^H}\downarrow H}(h) = \phi^H(h) \qquad (A16)$$

Assume that ϕ^H is an irreducible unitary representation of H. For a small representation $\phi^{G_{\phi^H}}$ of the little group G_{ϕ^H}, consider the induced representation $\phi^{G_{\phi^H}\uparrow G}$ of the group G. This representation is an irreducible unitary representation of G. Morever, all the irreducible unitary representations of G arise in this way.

Thus we see that the small representations of the little group are a crucial step in the construction of inequivalent irreducible unitary representations of a group G from the inequivalent irreducible unitary representations of a subgroup H. This construction is feasible only when the small representations of the little group can be obtained. One case where this is the case is when H is both a normal and abelian subgroup of G.

Suppose that H is both a normal and abelian subgroup of the group G, ϕ^H is an irreducible unitary representation of H, G_{ϕ^H} is the little group, and $\phi^{G_{\phi^H}}$ is a small representation of G_{ϕ^H}.

Using the definition of the little group G_{ϕ^H} and H a normal subgroup of G, we see that H is also a normal subgroup of G_{ϕ^H}. In particular, the quotient group G_{ϕ^H}/H is a subgroup of the quotient group G/H. For the left coset decomposition $G_{\phi^H} = \cup_i r_i H$, the quotient group G_{ϕ^H}/H has the multiplication law $r_1 r_2 = r_3(r_1, r_2)$ where $r_3(r_1, r_2)$ is the coset representative satisfying $r_1 r_2 H = r_3(r_1, r_2)H$. Note that while $r_1 r_2 = r_3(r_1, r_2)$ holds in the quotient group G_{ϕ^H}/H, only the weaker relation $r_1 r_2 = r_3(r_1, r_2)h_3(r_1, r_2)$ for some element $h_3(r_1, r_2)$ in H holds in the group G_{ϕ^H} itself.

Next consider the homomorphism relation $\phi^{G_{\phi^H}}(r_1)\phi^{G_{\phi^H}}(r_2) = \phi^{G_{\phi^H}}(r_1 r_2)$. By using $r_1 r_2 = r_3(r_1, r_2)h_3(r_1, r_2)$ and the homomorphism relation $\phi^{G_{\phi^H}}(r_3(r_1, r_2)h_3(r_1, r_2)) = \phi^{G_{\phi^H}}(r_3(r_1, r_2))\phi^{G_{\phi^H}}(h_3(r_1, r_2))$ we find

$$\phi^{G_{\phi^H}}(r_1)\phi^{G_{\phi^H}}(r_2) = \phi^{G_{\phi^H}}(r_3(r_1, r_2))\phi^{G_{\phi^H}}(h_3(r_1, r_2)) \qquad (A17)$$

Since $\phi^{G_{\phi^H}}$ is a small representation, $\phi^{G_{\phi^H}}(h_3(r_1, r_2)) = \phi^H(h_3(r_1, r_2))$ is a complex scalar.

Finally, we recognize

$$\phi^{G_{\phi^H}}(r_1)\phi^{G_{\phi^H}}(r_2) = \phi^H(h_3(r_1, r_2))\phi^{G_{\phi^H}}(r_3(r_1, r_2)) \qquad (A18)$$

as Eq. A7 for the defining relation for a projective unitary representation. Here the multiplication law is $r_1 r_2 = r_3(r_1, r_2)$ in the quotient group G_{ϕ^H}/H and the factor system is defined by $\phi^H(h_3(r_1, r_2))$ where $r_1 r_2 = r_3(r_1, r_2)h_3(r_1, r_2)$ in the group G_{ϕ^H}.

To summarize, when H is an abelian and normal subgroup of G, the inequivalent irreducible unitary representations can be constructed as follows. Find the inequivalent irreducible unitary representations ϕ^H of H. Divide the irreducible unitary representations ϕ^H into equivalence classes according to the relation $\phi_1^H \sim \phi_2^H$ if $\phi_1^H(h) = \phi_2^H(g^{-1}Hg)$ where g is an element of G.

For each equivalence class find the little group G_{ϕ^H} consisting of elements g that leave $\phi^H(h) = \phi^H(g^{-1}hg)$ fixed. Consider the quotient group G_{ϕ^H}/H which is itself a subgroup of the quotient group G/H. Here the multiplication law is $r_1 r_2 = r_3(r_1, r_2)$ in G_{ϕ^H}/H and $r_1 r_2 = r_3(r_1, r_2)h_3(r_1, r_2)$ in G_{ϕ^H} for $h_3(r_1, r_2)$ in H. Find the irreducible projective unitary representations $\psi^{G_{\phi^H}/H}$ that are projectively equivalent to the factor system $\phi^H(h_3(r_1, r_2))$.

Each of these projective unitary representations $\psi^{G_{\phi^H}/H}$ of G_{ϕ^H}/H can be extended to a unitary representation of G_{ϕ^H}. This can be seen as follows. For an arbitrary element g of G_{ϕ^H}, we can write the left coset decomposition $g = rh$ for some coset representative r and h an element of H. By taking $\psi^{G_{\phi^H}/H}(g) = \psi^{G_{\phi^H}/H}(r)\phi^H(h)$, we can use Eqs. A17 and A18 to show that $\psi^{G_{\phi^H}/H}(g_1 g_2) = \psi^{G_{\phi^H}/H}(g_1 g_2)$ satisfies the homomorphism relation.

Each of the induced representations $\psi^{G_{\phi^H}/H\uparrow G}$ is then an irreducible unitary representation of G. Each of these irreducible unitary representations is inequivalent for ϕ^H taken from different equivalence classes under the $\phi_1^H \sim \phi_2^H$ if $\phi_1^H(h) = \phi_2^H(g^{-1}Hg)$ for some g an element of G. By using all of the equivalence classes, all of the inequivalent irreducible unitary representations of G are obtained.

7. Anti-unitary co-representations

In order to have anti-unitary co-represenations, the group G must have a halving subgroup H. This means that H is an index two subgroup $|G|/|H| = 2$ of the group G. In particular, H is a normal subgroup and the quotient group G/H consists of two elements: the identity element $\mathbf{1}$ of G and a left coset representative z. The group G can be written as $G = H \cup zH$ with z satisfying

$$z \notin H, \qquad z^2 \in H, \qquad z^{-1}hz \in H \qquad (A19)$$

An anti-unitary co-representation ϕ_{AU} is a homomorphism from a group G to the group of complex linear and anti-linear unitary transformations. This means that for each group element h in H, $\phi_{AU}(h) = U(h)$ and for the element z in G, $\phi_{AU}(z) = U(z)\Theta$ where $U(h)$ and $U(z)$

are unitary matrices satisfying

$$U(h)^{-1} = U(h)^\dagger, U(z)^{-1} = U(z)^\dagger \qquad \text{(A20)}$$

and Θ is the complex conjugation operator. Here ϕ_{AU} is subject to the homomorphism condition

$$\phi_{AU}(g_1)\phi_{AU}(g_2) = \phi_{AU}(g_1 g_2) \qquad \text{(A21)}$$

In particular this implies

$$U(h_1)U(h_2) = U(h_1 h_2) \qquad U(z)U(z)^* = U(zz)$$
$$U(h)U(z)\Theta = U(hz), \qquad U(z)U(h)^*\Theta = U(zh) \quad \text{(A22)}$$

for the unitary matrices associated to the elements h, h_1, h_2 of the group H and element z of the group G. For a more detailed discussion of unitary representations and anti-unitary co-representations, see Ref. [20].

We now discuss how to construct the inequivalent irreducible anti-unitary co-representations ϕ_{AU}^G of G from the inequivalent irreducible unitary representations ϕ_U^H of the halving subgroup H. From Eq. A19, we know that $z^{-1}Hz = H$. This implies that since $\phi_U^H(h)$ is an irreducible unitary representation with h an element of the group H, $\phi_U^H(z^{-1}hz)^*$ with $*$ the complex conjugate is also an irreducible unitary representation of H. In particular, this means that there is a unitary matrix Z such that

$$\phi_U^H(z^{-1}hz)^* = Z^\dagger \varphi_U^H(h) Z \qquad \text{(A23)}$$

for some irreducible unitary representation φ_U^H of H.

From Eq. A19, notice z^2 is also an element of H. There are three cases two consider. The first case (1) is when ϕ_U^H and φ_U^H are inequivalent. The irreducible anti-unitary co-representation of G is given by

$$\phi_{AU}^G(h) = U(h) = \begin{bmatrix} \phi_U^H(h) & 0 \\ 0 & \varphi_U^H \end{bmatrix},$$

$$\phi_{AU}^G(h) = U(z)\Theta = \begin{bmatrix} 0 & \phi_U^H(z^2)Z^T \\ Z & 0 \end{bmatrix} \Theta \qquad \text{(A24)}$$

where T denotes the transpose and Θ is the complex conjugation operator.

The second case (2a) is when ϕ_U^H and φ_U^H are equivalent and $ZZ^* = -\phi_U^H(z^2)$. The irreducible anti-unitary co-representation of G is given by

$$\phi_{AU}^G(h) = U(h) = \begin{bmatrix} \phi_U^H(h) & 0 \\ 0 & \phi_U^H \end{bmatrix},$$

$$\phi_{AU}^G(h) = U(z)\Theta = \begin{bmatrix} 0 & -Z \\ Z & 0 \end{bmatrix} \Theta \qquad \text{(A25)}$$

where Θ is the complex conjugation operator.

The third case (2b) is when ϕ_U^H and φ_U^H are equivalent and $ZZ^* = +\phi_U^H(z^2)$. The irreducible anti-unitary co-representation of G is given by

$$\phi_{AU}^G(h) = U(h) = \phi_U^H(h), \quad \phi_{AU}^G(h) = U(z)\Theta = Z\Theta \tag{A26}$$

where Θ is the complex conjugation operator.

Notice that if ϕ_U^H is a $N \times N$ dimensional unitary representation, then ϕ_{AU}^G is a $2N \times 2N$ dimensional anti-unitary co-representation for cases (1) and (2a) while it is a $N \times N$ dimensional anti-unitary co-representation for case (2b). All of the inequivalent anti-unitary co-representations ϕ_{AU}^G of G are obtained by using the above procedure once for each pair of type (3) inequivalent irreducible unitary representations ϕ_U^H, φ_{AU}^H of H and once for each type (2a) or (2b) inequivalent irreducible unitary representation ϕ_U^H of H

The construction of the unitary matrix Z is described in Ref. [20]. Consider the projectors

$$P_i = \frac{N}{|H|} \sum_h \phi_U^H(h)_{1i} \phi_U^H(z^{-1}hz)^T \qquad \text{(A27)}$$

where $N \times N$ is the dimensionality of ϕ_U^H, $|H|$ is the order or number of elements in the group H, and $\phi_U^H(h)_{1i}$ is the $(1, i)$ scalar matrix element of $\phi_U^H(h)_{1i}$. Let x be the unique normalized column eigenvector x with eigenvalue one for P_1. Then the i row of Z is given by $x^\dagger P_i^\dagger$.

8. Real orthogonal representations

A real orthogonal representation ϕ_O is a homomorphism from a group G to the group of linear orthogonal transformations. This means that for each group element g in G, $\phi_O(g) = O$ where O is a finite-dimensional real orthogonal matrix satisfying

$$O(g)^* = O(g), \qquad O(g)^{-1} = O(g)^T \qquad \text{(A28)}$$

where $*$ denotes complex conjguation and T denotes the transpose. Here, ϕ_O is subject to the homomorphism condition

$$\phi_O(g_1)\phi_O(g_2) = \phi_O(g_1 g_2) \qquad \text{(A29)}$$

for each element g', g in the group G. In particular, this implies

$$O(g_1)O(g_2) = O(g_1 g_2) \qquad \text{(A30)}$$

for the orthogonal matrices associated to the elements g', g in the group G

We are primarily interested in the three-dimensional real orthogonal representations of space groups for the analysis of spin groups. Luckily, the three-dimensional real orthogonal representations can be easily obtained from the two-dimensional complex unitary representations and anti-unitary co-representations. Physically, this corresponds to using two component complex unit spinors to construct three component real vectors. Mathematically, it corresponds to the 2-to-1 homomorphism from $SU(2)$ to $SO(3)$.

When U is a two-dimensional complex unitary matrix

$$O_U^{ij}(U) = \frac{1}{2}\text{Tr}\left[\sigma^i U^\dagger \sigma^j U\right] \qquad \text{(A31)}$$

is a three-dimensional real orthogonal matrix. Similarly, when $U\Theta$ is a two-dimensional complex anti-unitary matrix

$$O_{AU}^{ij}(U) = \frac{1}{2}\text{Tr}\left[\sigma^i U^T(\sigma^j)^T U^*\right] \qquad \text{(A32)}$$

is a three-dimensional real orthogonal matrix. In both of the above, σ^i are the Pauli matrices. Using the completeness relation for Pauli matrices

$$\sum_i \sigma^i_{\alpha\beta}\sigma^i_{\gamma\delta} = 2\delta_{\alpha\delta}\delta_{\beta\gamma} - \delta_{\alpha\beta}\delta_{\gamma\delta} \qquad \text{(A33)}$$

we can show that

$$O_U^{ij}(U_1)O_U^{ij}(U_2) = O_U^{ij}(U_1 U_2),$$
$$O_{AU}^{ij}(U_1)O_{AU}^{ij}(U_2^*) = O_U^{ij}(U_1 U_2)$$
$$O_U^{ij}(U_1)O_{AU}^{ij}(U_2) = O_{AU}^{ij}(U_1 U_2),$$
$$O_{AU}^{ij}(U_1)O_U^{ij}(U_2^*) = O_{AU}^{ij}(U_1 U_2), \qquad \text{(A34)}$$

satisfies that appropriate homomorphism relations.

Appendix B: Cyclic, dihedral, and double dihedral groups

In two dimensions, point groups are either cyclic C_n or dihedral D_n. Here we discuss the structure of these groups, their subgroups, their inequivalent irreducible unitary representations, and their projectively inequivalent irreducible projective unitary representations.

Cyclic groups have generators that satisfy $r^n = s = \mathbf{1}$ with n group elements r^m where $m = 0\dots n-1$ and $\mathbf{1}$ is the identity element. These groups are abelian and the inequivalent irreducible complex unitary representations are one-dimensional and labeled by an integer $\mu = 0\dots n-1$. For the generator r, the representation is given by

$$\phi_\mu^{C_n}(r) = \exp(2\pi i\mu/n), \qquad \text{(B1)}$$

with the homomorphism relation $\phi_\mu^{C_n}(r^m) = \phi_\mu^{C_n}(r)^m$ specifying the representation for the entire group. The projective inequivalent irreducible projective unitary representations of C_n are projectively equivalent to the complex unitary representations of C_n with trivial factor system.

For the cyclic group C_n of order n, the subgroups are also cyclic C_p^n of order p where p is a divisor of n. There are p elements of C_p^n given by the elements $r^{qn/p}$ of the group C_n for $q = 0\dots p-1$. The left coset decomposition of the group C_n is given by $C_n = \cup_r r^u C_p^m$ with left coset representatives r^u where $u = 0\dots n/p-1$.

Dihedral groups have generators that satisfy $r^n = s^2 = \mathbf{1}$ with $2n$ group elements $r^m s^t$ with $m = 0\dots n-1$ and $t = 0,1$ and $\mathbf{1}$ is the identity element. Such groups are non-abelian except for $n \leq 2$. For the generators

	Rep.	r	s
n odd	A_0	$+1$	$+1$
	A_1	$+1$	-1
	E_μ	$\exp(2\pi i\mu\sigma^y/n)$	σ^z
n even	A_0	$+1$	$+1$
	A_1	$+1$	-1
	B_0	-1	$+1$
	B_1	-1	-1
	E_μ	$\exp(2\pi i\mu\sigma^y/n)$	σ^z

TABLE III: The inequivalent irreducible unitary representations $\phi_{Rep}^{D_n}$ for the generators r, s of the dihedral group D_n. Here $\mu = 1\dots n/2 - 1$ for n even, $\mu = 1\dots (n-1)/2$ for n odd, and σ^i are the Pauli matrices.

r, s, the inequivalent irreducible unitary representations are given by Table III with the homomorphism relation $\phi_{Rep}^{D_n}(r^m s^t) = \phi_{Rep}^{D_n}(r)^m \phi_{Rep}^{D_n}(s)^t$ specifying the representation for the entire group.

For the dihedral group D_n of order n, the subgroups are one of two types. The first is cyclic C_p^n of order p where p is a divisor of n. There are p elements of C_p^n given by the elements $r^{qn/p}$ of the group D_n for $q = 0\dots p-1$. The left coset decomposition of the group D_n is given by $D_n = \cup_{r,t} r^u s^v C_p^m$ with $2n/p$ left coset representatives $r^u s^v$ where $u = 0\dots n/p-1$ and $v = 0,1$.

The second is dihedral $D_{p,\nu}^n$ of order p where p is a divisor of n and $\nu = 0\dots n/p-1$. There are $2p$ elements of $D_{p,\nu}^n$ given by the elements $r^{qn/p+u\nu}S^t$ of the group D_n for $q = 0\dots p-1$ and $u = 0,1$. The left coset decomposition of the group D_n is given by $D_n = \cup_r r^v D_{p,\nu}^n$ with n/p left coset representatives r^v where $v = 0\dots n/p-1$.

The projectively inequivalent irreducible projective unitary representations of D_n are most easily obtained from the inequivalent irreducible unitary representations of the double dihedral group D_n' with $4n$ group elements $r^m s^t e^u$ where $m = 0\dots n-1$, $t = 0,1$, and $u = 0,1$. The generators of the double dihedral group satisfy $r'^n = s'^2 = e'$ with $e'^2 = \mathbf{1}$ where $\mathbf{1}$ is the identity element. For the generators r', s', e', the inequivalent irreducible unitary representations are given by Table IV with the homomorphism relation $\phi_{Rep}^{D_n'}(r'^m s'^t e'^u) = \phi_{Rep}^{D_n'}(r')^m \phi_{Rep}^{D_n'}(s')^t \phi_{Rep}^{D_n'}(e')^u$ specifying the representation for the entire group.

When n is odd, the projectively inequivalent irreducible projective unitary representations of D_n are projectively equivalent to the complex unitary representations of D_n with trivial factor system. When n is even, it is convenient to introduce the function f which embeds the dihedral group D_n into the double dihedral group D_n' via $f(R^m S^s) = R'^m S'^s$. The projectively inequivalent irreducible projective unitary representations of D_n are projectively equivalent to $\phi^{D_2}(g) = \phi^{D_2'}(f(g))$ where g is an element in D_n and the factor system is $\lambda(g_1, g_2) = \phi^{D_2'}(f(g_1 g_2)^{-1} f(g_1) f(g_2))$. This factor sys-

	Rep.	r'	s'	e'
n odd	A_0	$+1$	$+1$	$+1$
	A_1	$+1$	-1	$+1$
	B_0	-1	$+i$	-1
	B_1	-1	$-i$	-1
	E_μ	$\exp(\pi i\mu\sigma^u/n)$	$i^\mu\sigma^z$	$(-1)^\mu\sigma^0$
n even	A_0	$+1$	$+1$	$+1$
	A_1	$+1$	-1	$+1$
	B_0	-1	$+1$	$+1$
	B_1	-1	-1	$+1$
	E_μ	$\exp(\pi i\mu\sigma^u/n)$	$i^\mu\sigma^z$	$(-1)^\mu\sigma^0$

TABLE IV: The inequivalent irreducible unitary representations $\phi_{Rep}^{D'_n}$ for the generators r', s', e' of the double dihedral group D'_n. Here $\mu = 1\ldots n-1$, σ^i are the Pauli matrices, and σ^0 is the identity matrix.

tem is projectively equivalent to the trivial factor system when $\phi^{D'_n}(E') = +1$. It is a non-trivial factor system for $\phi^{D'_n}(E') = -1$ which occurs for the E_μ irreducible unitary representations of D'_n with n even and μ odd.

Appendix C: Representation theory approach to spin groups

Here we compare the implicit classification of spin groups presented in Litvin and Opechowski [14] and the constructive approach in Section IV using the representation theory of space groups.

Litvin and Opechowski use a result classifying subgroups of direct product groups originally due to Zamorzaev [21]. Consider the direct product $\mathbf{B} \otimes \mathbf{F}$ of groups $\mathbf{B}$, $\mathbf{F}$. An element of $\mathbf{B} \otimes \mathbf{F}$ is given by (B, F) and the identity, product, and inverse are given by $(\mathbf{1}_B, \mathbf{1}_F)$, $(B', F')(B, F) = (B'B, F'F)$, $(B, F)^{-1} = (B^{-1}, F^{-1})$, where $\mathbf{1}_{B,F}$ is the identity element in $\mathbf{B}$, $\mathbf{F}$.

Denote a subgroup of $\mathbf{B} \otimes \mathbf{F}$ by X. For all elements of X consisting of elements of the form (B, F), drop F to obtain $\mathcal{B}$, a subgroup of $\mathbf{B}$. For all elements of X consisting of elements of the form (B, F), drop B to obtain $\mathcal{F}$, a subgroup of $\mathbf{F}$. For all elements of X consisting of elements of the form $(B, \mathbf{1}_F)$, drop $\mathbf{1}_F$ to obtain a normal subgroup b of $\mathcal{B}$. For all elements of X consisting of elements of the form $(\mathbf{1}_B, F)$, drop $\mathbf{1}_B$ to obtain a normal subgroup f of $\mathcal{F}$. Litvin and Opechowski call X in the family of $\mathcal{B}$ and $\mathcal{F}$. The result of Zamorzaev states that the quotient groups $\mathcal{B}/b$ and $\mathcal{F}/f$ are isomorphic.

Subgroups X of $\mathbf{B} \otimes \mathbf{F}$ are thus classified by a normal subgroup b of $\mathcal{B}$ the latter of which is a subgroup of $\mathbf{B}$, a normal subgroup f of $\mathcal{F}$ the latter of which is a subgroup of $\mathbf{F}$, and an isomorphism ψ from $\mathcal{B}/b$ from $\mathcal{F}/f$.

The connection between the Litvin and Opechowski approach and the representation theory approach is given by the first isomorphism theorem [19]. For a homomor-

phism φ from group G to group H, the first isomorphism theorem states that (1) $\ker(\varphi)$ is a normal subgroup of G, (2) $\mathrm{im}(\varphi)$ is a subgroup of H, and (3) $\mathrm{im}(\varphi)$ is isomorphic to the quotient group $G/\ker(\phi)$.

Spin groups are subgroups of the direct product group $E(2) \otimes O(3)$ with $E(2)$ the two-dimensional Euclidean group of real-space operations and $O(3)$ the three-dimensional orthogonal group of spin-space operations. Recall that within the representation theory approach, spin groups are given by a choice of space group SG with elements (M, t), a choice of a three-dimensional orthogonal representation ϕ, and N is a group that satisfies $\phi(M, t)^{-1} N \phi(M, t) = N$.

Let us take $b = \ker(\phi)$, $\mathcal{B} = SG$, $\mathbf{B} = E(2)$, and $f = N$, $\mathcal{F} = \mathrm{im}(\phi)N = N\mathrm{im}(\phi)$, $\mathbf{F} = O(3)$. From (1) of the first isomorphism theorem, b is a normal subgroup of $\mathcal{B}$ and we already know that SG is a subgroup of $E(2)$. By construction f is a normal subgroup of $\mathcal{F}$ the latter of which is a subgroup of $\mathbf{F}$. The quotient group $\mathcal{F}/f$ is the image $\mathrm{im}(\phi)$ while $\mathcal{B}/b$ is the kernel $\ker(\phi)$. From (3) of the first isomorphism theorem, we see that $\mathcal{B}/b$ and $\mathcal{F}/f$ are isomorphic.

Thus we see that given SG, N, and ϕ within the representation theory approach, we can construct b, $\mathcal{B}$, f, $\mathcal{F}$ within the Litvin-Opechowski approach. If instead we are given b, $\mathcal{B}$, f, $\mathcal{F}$, we can again use the first isomorphism theorem to construct SG, N, and ϕ.

Appendix D: Unitary representations and anti-unitary co-representations of space groups

In this appendix, we outline the construction of the unitary representations and anti-unitary co-representations of space groups. We will use the results of Appendix A 6 on small representations and little groups and representation theory as well as the results of Appendix B on point groups in two dimensions.

Recall from Section IV that an element (M, t) of a two-dimensional space group SG consists of a 2×2 orthogonal matrix M describing rotations/reflections and a two-component vector t describing translations. It acts on a point x via

$$x_\mu \to M_{\mu\nu} x_\nu + t_\mu \tag{D1}$$

and the product satisfies

$$(M', t')(M, t) = (M'M, M't + t') \tag{D2}$$

where M describes the action of the point group PG and t the action of the translations T. In particular, this implies

$$(M, t)^{-1} = (M^{-1}, -M^{-1}t),$$
$$(M', t')^{-1}(M, t)(M', t') = (M'^{-1}MM', M'^{-1}(Mt' + t - t')) \tag{D3}$$

for the inverse element and conjugate action of the element (M, t) by the element (M', t'), respectively.

The translation subgroup T consists of elements $(\mathbf{1}, t)$ with $\mathbf{1}$ the identity matrix. It is an abelian group with generators $T_1 = (\mathbf{1}, t_1)$, $T_2 = (\mathbf{1}, t_2)$. From the above, conjugation of $(\mathbf{1}, t)$ by (M', t') yields $(\mathbf{1}, M'^{-1}t)$. This implies T is a normal subgroup of SG and the quotient group SG/T is called the point group PG. It is either a cyclic or dihedral group of order $n = 1, 2, 3, 4, 6$ as described in Appendix B.

Since T is a normal and abelian subgroup of SG, we will use the results of Appendix A 6 to construct the inequivalent irreducible unitary representations. The inequivalent irreducible representations of T are labeled by a wavevector $k = \gamma k_1 + \delta k_2$ where k_i are basis vectors for the reciprocal lattice satisfying $k_i \cdot t_i = \delta_{ij}$ with $\cdot$ the dot product. This representation is given by

$$\phi_k^T(T_1^c T_2^d) = \exp[-2\pi i k \cdot (ct_1 + dt_2)] = \exp[-2\pi i(\gamma c + \delta d)] \tag{D4}$$

where k is restricted to the first Brioullin zone.

The conjugate action is given by $\phi_k^T((M,t)^{-1} T_1^c T_2^d (M,t)) = \phi_{Mk}^T(T_1^c T_2^d)$ from which we can see that it is equivalent to the rotation/reflection M acting directly on the wavevector k. Under the equivalence relation defined by this conjugate action, k and Mk are in the same class. These classes divide the Brioullin zone into $|PG|$ regions with $|PG|$ the order of the point group. We then choose one k as a representative for each class.

For each of these k, consider the little group SG_k given by the subgroup of SG with elements (M, t) that leave ϕ_k^T fixed under the conjugate action. Since the conjugate action takes ϕ_k^T to ϕ_{Mk}^T, this implies that (M, t) is in the little group SG_k if Mk and k differ by a reciprocal lattice vector.

The quotient group SG_k/T is a subgroup of the quotient group SG/T. Since the latter is the point group $SG/T = PG$, we will refer to the former as the wavevector point group $SG_k/T = PG_k$. In Appendix B, we list the two-dimensional point groups PG and their possible subgroups. From I, we list the group elements (M, t) for the point group generators R, S. This allows us to obtain the left coset representatives r_i for the left coset decomposition $SG = \cup_i r_i SG_k/T$, the multiplication law $r_1 r_2 = r_3(r_1, r_2)$ for the quotient group SG_k/T, and the multiplication law $r_1 r_2 = r_3(r_1, r_2) h_3(r_1, r_2)$ for the group SG where $h_3(r_1, r_2)$ is an element of the translation group T.

This then gives the factor system $\phi_k^T(h_3(r_1, r_2))$. We list the possible projective representations which $\phi_k^T(h_3(r_1, r_2))$ is projectively equivalent to in Appendix B. The irreducible projective unitary representations $\psi_{Rep}^{PG_k}$ that arise give an irreducible unitary representation of SG_k. The induced representation $\psi_{Rep}^{PG_k \uparrow SG}$ is an irreducible unitary representation of SG. Choosing one k as a representative for the equivalence classes defined by the relation $k \sim Mk$ gives all of the inequivalent irreducible unitary representations of SG.

For a given space group SG, it is useful to consider two types of space groups derived from SG in the construction of anti-unitary co-representations: grey space groups SG^{Grey} and black-white space groups SG^{BW}. We first introduce the element τ that commutes with all elements of SG and satisfies $\tau^2 = \mathbf{1}$ with $\mathbf{1}$ the identity element. A physical interpretation for τ is as the time-reversal operator.

A grey space group is given by the left coset decomposition $SG^{Grey} = SG \cup \tau SG$. It has double the number of elements of the original space group SG the latter of which is a halving subgroup of SG^{Grey}. We have already discussed how the inequivalent irreducible unitary representations of a space group SG are constructed. For a grey space group $SG^{Grey} = SG \cup \tau SG$, we can use the results of Appendix A 7 with the group $G = SG^{Grey}$ and halving subgroup $H = SG$ to then construct the inequivalent irreducible anti-unitary co-representations.

A black-white space group is given by the left coset decomposition $SG^{BW} = SG^{1/2} \cup \tau z SG^{1/2}$. It has the same number of elements as the original space group SG. Here SG itself has a halving subgroup $SG^{1/2}$ and left coset decomposition $SG = SG^{1/2} \cup z SG^{1/2}$ where z is the left coset representative. Given the inequivalent irreducible unitary representations of the halving space group $SG^{1/2}$, we can again use Appendix A 7 to construct the inequivalent irreducible anti-unitary co-representations.

For each space group SG, we see there is only one grey space group SG^{Grey}. However, there can be multiple inequivalent halving subgroups $SG^{1/2}$ for SG and thus multiple black-white space groups SG^{BW} for SG. Here two halving subgroups $SG^{1/2}$ and $SG^{1/2\prime}$ of SG are equivalent if they are related conjugation by a fixed element (M, t) of the larger $E(2)$ Euclidean group $SG^{1/2\prime} = (M, t)^{-1} SG^{1/2}(M, t)$. Tables of inequivalent halving space groups for each space group SG are given in Ref. [17].

For black-white space groups, we see that each element (M, t) of the space group SG is associated with either the element (M, t) or $\tau(M, t)$ (but not both) in the black-white space group SG^{BW}. Here the nomenclature of black-white space group becomes clear since for (M, t) in SG we can associate the color white if it corresponds to (M, t) in SG^{BW} and black if it corresponds to $\tau(M, t)$ (or vice versa). For grey space groups, we see that each element (M, t) of the space group SG is associated with both of the elements (M, t) and $\tau(M, t)$ in the grey space group SG^{Grey}. Using the same nomenclature, each (M, t) in SG is black and white and associated with the color grey.

There is one difficulty in construction of the anti-unitary co-representations of a grey SG^{Grey}, or black-white space group SG^{BW} from the unitary representations of the appropriate halving space group SG. This lies in the calculation of the unitary matrix Z since one must be careful in defining the sum over the halving space group SG which is infinite. Here it is useful to use the left coset decomposition of SG by the translation subgroup

T given by $SG = \cup_i r_i SG/T$ where r_i are left coset representatives of the quotient group SG/T which is given by the point group. This allows us to write $\sum_{SG} = \sum_{r_i} \sum_T$. The summation over r_i corresponds to a summation over the point group which is finite and well-defined. The summation over the translation group T corresponds to a discrete Fourier transform. Although it is formally an infinite sum, it physically corresponds to projection of the summand onto the zero wavevector component which is well-defined.

Appendix E: Spin group for the minimal energy spin texture

Here we present the construction of the spin group for the minimal energy spin texture. This particular spin group is constructed from an anti-unitary co-representation of a black-white space group. It offers a illustration of the construction of irreducible unitary representations and anti-unitary co-representations of space groups and their use in the construction of spin groups.

The space group is given by $p2mg$ with the normal subgroup of translations given by a rectangular Bravais lattice T_{Rect} with generators given by

$$T_1 = (\mathbf{1}, [a, 0]), \qquad T_2 = (\mathbf{1}, [0, b]) \qquad (E1)$$

where a, b are the lattice constants and $\mathbf{1}$ is the 2×2 identity matrix. The point group given by the quotient group $p2mg/T_{Rect}$ is the dihedral group D_2 of order $n = 2$. This space group is non-symmorphic with generators for rotations R and reflections S given by

$$R = (-\mathbf{1}, [0, 0]), \qquad S = (-\sigma^z, [a/2, 0]) \qquad (E2)$$

where σ^z is a Pauli matrix and notice that S has an associated non-trivial translation.

One of the halving space groups for $p2mg$ is given by the $p2gg$ space group. It also has a rectangular Bravais lattice $T_{Rect}^{1/2}$ with generators given by

$$T_1^{1/2} = (\mathbf{1}, [a, 0]), \qquad T_2^{1/2} = (\mathbf{1}, [0, 2b]) \qquad (E3)$$

where the lattice constant for the $T_2^{1/2}$ element of the halving space group $p2gg$ is twice that of T_2 for the space group $p2mg$. Notice in particular that the element T_2 of the space group $p2mg$ is not an element of the halving space group $p2gg$. The point group given by the quotient group $p2gg/T_{Rect}^{1/2}$ is also the dihedral group D_2 of order $n = 2$. This halving space group is also non-symmorphic with generators for rotations $R^{1/2}$ and reflections $S^{1/2}$ given by

$$R^{1/2} = (-\mathbf{1}, [0, 0]), \qquad S^{1/2} = (-\sigma^z, [a/2, b]) \qquad (E4)$$

where σ^z is a Pauli matrix and notice that S has an associated non-trivial translation. The left coset decomposition of the space group $p2mg$ by the halving space

group $p2gg$ is given by $p2mg = p2gg \cup T_2 p2gg$. Here the left coset representative is given by T_2. The corresponding black-white space group is $p(2b)m'g'$ in the notation of Ref. [17].

We now turn to the construction of one of the inequivalent irreducible unitary representations of the halving space group $p2gg$ using the procedure described in Appendix A 6 and D. The wavevector specifying the irreducible unitary representation of the translation subgroup $T_{Rect}^{1/2}$ of the halving space group $p2gg$ for the minimal energy spin group is given by the wavevector $k = k_1/2$ where $k_2 = (2\pi/a, 0)$ is a reciprocal lattice vector. Explicitly, the representation is given by

$$\phi_{k_1/2}^{T_{Rect}^{1/2}}((T_1^{1/2})^c (T_2^{1/2})^d) = \exp[-\pi i c] \qquad (E5)$$

where a general element $t = (T_1^{1/2})^c (T_2^{1/2})^d$ of the translation group $T^{1/2}$ is expressed as c, d powers of the generators $T_1^{1/2}$, $T_1^{1/2}$.

Conjugation by the generators $R^{1/2}$, $S^{1/2}$ of the D_2 point group for the halving space group $p2gg$ leaves $\phi_{k_2/2}^{T_{Rect}^{1/2}}$ fixed. Since conjugation by $T_1^{1/2}$ and $T_2^{1/2}$ also leaves $\phi_{k_1/2}^{T_{Rect}^{1/2}}$ fixed, we see that the little group $p2gg_{k_1/2}$ for the $k = k_1/2$ representation of the translation subgroup $T_{Rect}^{1/2}$ of the halving subgroup $p2gg$ is given by $p2gg$ itself.

The quotient group $p2gg_{k_1/2}/T_{Rect}^{1/2} = D_2$ of the little group by the translation subgroup is the D_2 point group. Consider the element $R^{1/2} S^{1/2} = (+\sigma^z, [a/2, b])$. For the quotient group $p2gg_{k_1/2}/T_{Rect}^{1/2} = D_2$ we see the multiplication law is $R^{1/2} S^{1/2} R^{1/2} S^{1/2} = \mathbf{1}$. In $p2gg_{k_1/2}$ itself, the multiplication law is $R^{1/2} S^{1/2} R^{1/2} S^{1/2} = T_1^{1/2}$. Since $\phi_{k_1/2}^{T_1^{1/2}}(T_2^{1/2}) = -1$ is non-trivial, we see that we require one of the projectively inequivalent irreducible projective unitary representations of $p2gg/T_{Rect}^{1/2} = D_2$ with non-trivial factor system.

From Appendix D, we see there is only one such projective unitary representation of D_2 given by the E_1 unitary representation of D_2' in Table IV. Labeling this projective representation as $\psi_{E_1}^{p2gg_{k_1/2}/T_{Rect}^{1/2}}$, we see it gives one of the inequivalent irreducible unitary representations of the little group $p2gg_{k_1/2}$. Since $p2gg_{k/1/2} = p2gg$ is the halving subgroup $p2gg$ itself, the induced representation $\psi_{E_1}^{p2gg_{k_1/2}/T_{Rect}^{1/2} \uparrow p2gg}$ is simply $\psi_{E_1}^{p2gg_{k_1/2}/T_{Rect}^{1/2}}$. Thus we obtain one of the inequivalent irreducible unitary representations of the halving subgroup $p2gg$. Labeling this representation as $\phi_{k_1/2, E_1}^{p2gg}$, we find for the generators

$$\phi_{k_1/2, E_1}^{p2gg}(T_1^{1/2}) = -\sigma^0, \qquad \phi_{k_1/2, E_1}^{p2gg}(T_2^{1/2}) = +\sigma^0,$$
$$\phi_{k_1/2, E_1}^{p2gg}(R^{1/2}) = \sigma^y, \qquad \phi_{k_1/2, E_1}^{p2gg}(S^{1/2}) = \sigma^z \qquad (E6)$$

where $\mathbf{1}$ is the 2×2 identity matrix and σ are the Pauli matrices.

Using this irreducible unitary representation of the halving subgroup $p2gg$, We now turn to the construction of one of the inequivalent irreducible anti-unitary representations of the space group $p2gg$ using the procedure described in Appendix A 7 and D. The left coset decomposition of $p2mg = p2gg \cup T_2 p2gg$ has left coset representative T_2. The conjugate action of T_2 is given by

$$T_2^{-1} T_1^{1/2} T_2 = T_1^{1/2}, \qquad T_2^{-1} T_2^{1/2} T_2 = T_2^{1/2},$$
$$T_2^{-1} R^{1/2} T_2 = R^{1/2} T_2^{1/2}, \quad T_2^{-1} S^{1/2} T_2 = S^{1/2}, \qquad \text{(E7)}$$

on the generators of the halving subgroup $p2gg$. We can check that

$$\phi_{k_1/2, E_1}^{p2gg}(T_2^{-1} h T_2^{-1})^* = \sigma^z \phi_{k_1/2, E_1}^{p2gg}(h) \sigma^z \qquad \text{(E8)}$$

for each of the elements h of the halving subgroup $p2gg$. This implies that the the unitary matrix $Z = \sigma^z$ with $ZZ^* = +1$ and the resulting anti-unitary co-representation is of type (2b). Labeling this anti-unitary co-representation as $\phi_{k_1/2, E_1, AU}^{p2mg}$, we find for the generators

$$\phi_{k_1/2, E_1, AU}^{p2mg}(T_1) = -\sigma^0, \quad \phi_{k_1/2, E_1, AU}^{p2mg}(T_2) = +\sigma^0 \Theta,$$
$$\phi_{k_1/2, E_1, AU}^{p2mg}(R) = \sigma^y, \qquad \phi_{k_1/2, E_1, AU}^{p2mg}(S) = \sigma^z \Theta \quad \text{(E9)}$$

where Θ is the complex conjugation operator.

Using the results of Appendix A 8, we can then calculate the corresponding real orthogonal representation labelled as $\phi_{k_1/2, E_1, Orth}^{p2gg}$. We find for the generators

$$\phi_{k_1/2, E_1, Orth}^{p2mg}(T_1) = \text{Diag}[+ + +],$$
$$\phi_{k_1/2, E_1, Orth}^{p2mg}(T_2) = \text{Diag}[- + +],$$
$$\phi_{k_1/2, E_1, Orth}^{p2mg}(R) = \text{Diag}[- + -],$$
$$\phi_{k_1/2, E_1, Orth}^{p2mg}(S) = \text{Diag}[+ - +] \qquad \text{(E10)}$$

where $\text{Diag}[s_1 s_2 s_3]$ denotes the 3×3 diagonal matrix with entries s_i on the diagonal. The corresponding spin group is associated with the minimal energy spin texture and is also shown in Table II.

Appendix F: Construction of compatbile spin groups

In this section, we discuss the construction of the list compatible spin groups in Table II. In Section IV of the main text, we have already argued that the constraints in Section III allow us to consider spin groups with real space operations given by space groups with a T_{Rect} rectangular Bravais lattice and D_2 point group. This implies that the space group SG is either $p2mm$, $p2mg$, or $p2gg$. In addition, the subgroup of global spin space operations N has to be the trivial group. Here we discuss how to find all of the unitary representations and anti-unitary co-representations that give rise to real orthogonal representations describing spin space operations for spin groups.
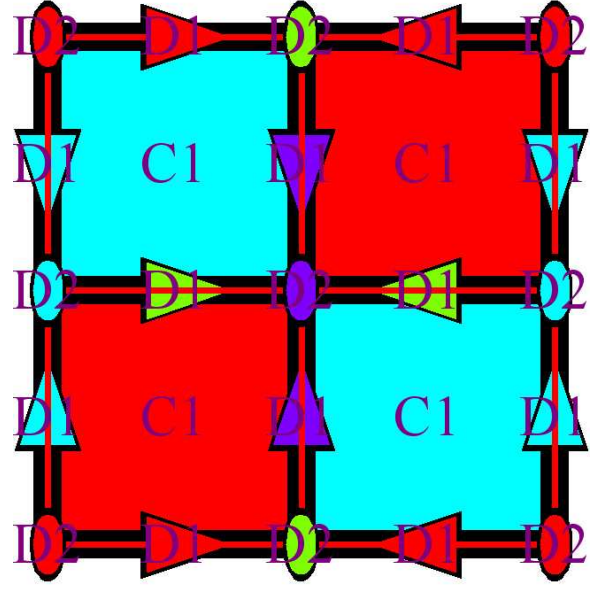

FIG. 4: (Color online) Brioullin zone for a space group SG with rectangular Bravais lattice T_{Rect} and $SG/T_{Rect} = D_2$ point group. Each wavevector k in the Brioullin zone describes an inequivalent and irreducible representation ϕ_k of the translation group T_{Rect}. The little group SG_k consists of elements of SG that leave ϕ_k fixed under conjugation. The wavevector point group SG_k/T_{Rect} is the trivial group C_1 for a generic wavevector in the Brioullin zone, D_1 on high symmetry lines, and D_2 on high symmetry points.

Let us first consider spin group arising from unitary representations of space groups. From Appendix D, for each space group SG we first consider all wavevectors k which give rise to irreducible and inequivalent representations ϕ_k of T_{Rect}. This is given by the first Brioullin zone is shown for T_{Rect} in Fig. 4.

Choosing one wavevector k out of each set of wavevectors related by a point group operation, we then construct the wavevector point group $PG_k = SG_k/T_{Rect}$ given by the quotient group of the little group SG_k leaving ϕ_k fixed under conjugation by T_{Rect}. We then find all of the projectively inequivalent projective representations $\psi_{Rep}^{PG_k}$ of $PG_k = SG_k/T_{Rect}$ and then construct the induced representation $\psi_{Rep}^{PG_k \uparrow SG}$. This gives all of the inequivalent and irreducible unitary representations of SG.

Notice as k varies continuously throughout the first Brioullin zone, ϕ_k varies continuously. However, PG_k changes discontinuously from the trivial group for a generic point to D_1 on high symmetry lines and D_2 on high symmetry points. This means that although individual matrix elements of the unitary representations of SG depend continuously on k, the underlying structure of the unitary representation such as locations of non-zero matrix elements and dimensionality only change discontinuously at high symmetry lines and points. This

makes it possible enumerate all of inequivalent and irreducible unitary representations of SG by treating all of the generic wavevectors k together and all of the wavevectors k on each of the high symmetry lines together.

It can be shown that dimensionality of the unitary representation of SG at a generic wavevector k is given by the order of the point group PG. For D_2, the order or number of elements is four which implies that we cannot use it to construct a three-dimensional real orthogonal representation. At high symmetry points and lines, the dimensionality of the unitary representation of SG can be smaller and if it is equal to two, it gives rise to a three-dimensional real orthogonal representation which can be used to construct a spin group. Furthermore, it can also be shown that tuning k on high symmetry lines tunes an incommensurate spin modulation between unit cells living on top of short length scale modulations within each unit cell. On physical grounds we expect the shorter length scale modulations to capture most of the gains in dipolar interaction energy. Alternatively, a specific value of k on high symmetry lines is selected based on energetics and we expect that minima occur at the boundaries corresponding to the high symmetry points. From these above arguments, we focus solely on the two-dimensional unitary representations arising from high symmetry points.

For each of these two-dimensional unitary representations, we then consider the actions of the corresponding spin groups on the magnetization and skyrmion charge in real space and momentum space as described in Section IV. The spin groups that do not force the magnetization to vanish at some point but force the net magnetization and net skyrmion charge to vanish are then compatible spin groups. There are only two compatible spin groups arising from unitary representations of space groups and are the first ones shown in Table II for the $p2mg$, $p2gg$ space groups. The corresponding wavevector k, wavevector point group PG_k and projective representation ψ^{PG_k} are specified as well. The projective representations use the notation of Appendix B.

Now we consider spin groups arising from anti-unitary co-representations of space groups. From D, for each space group SG we have to consider the grey space group SG^{Grey} and each of the black-white space groups SG^{BW} arising from each of the inequivalent halving subgroups $SG^{1/2}$ of SG. We can rule out the grey space group SG^{Grey} because this gives rise to a non-trivial global spin symmetry operation. For each of the SG^{BW}, we have to first construct the unitary representations of the halving space groups. This follows from the same procedure described above but we have to keep track of both two-dimensional and one-dimensional unitary representations of $SG^{1/2}$. This is because it is possible to construct two-dimensional anti-unitary co-representations of SG from one two-dimensional unitary representation of $SG^{1/2}$ or a pair of one-dimensional unitary representations of $SG^{1/2}$.

Applying the constraints coming from the real space and momentum space actions of spin groups gives the remaining compatible spin groups in Table II. The name of the black-white space group $BWSG$ in the notation of Ref. [17], the halving space group $SG^{1/2}$ are also included. The corresponding wavevector k, wavevector point group PG_k and projective representation ψ^{PG_k} for the halving space group $SG^{1/2}$ (not the space group SG) are specified as well. The projective representations use the notation of Appendix B.

Appendix G: Spin texture spherical interpolation

The low-energy effective theory we consider is defined in terms of a three-component unit vector $\hat{n}(x)$ which lives on the sphere in spin-space. To numerically calculate the energy, it is necessary to discretize the spin texture. In order to accurately describe a smooth spin texture, it is desirable to interpolate between the discretized values before calculating the energy.

In this section, we consider the problem of spherical interpolation between discrete samples of $\hat{n}(x)$. We take the spin texture to be in the symmetry class described by a spin group with basis vectors t_1 and t_2 and consider a $N_1 \times N_2$ discretization given by

$$\hat{n}(u_1, u_2) = \hat{n}(u_1 t_1/N_1 + u_2 t_2/N_2) \qquad (G1)$$

where $0 \leq u_i < N_i$. Given samples on the corners of a plaquette

$$\begin{bmatrix} \hat{n}(0.0, 1.0) & \hat{n}(1.0, 1.0) \\ \hat{n}(0.0, 0.0) & \hat{n}(1.0, 0.0) \end{bmatrix} \rightarrow$$

$$\begin{bmatrix} \hat{n}(0.0, 1.0) & \hat{n}(0.5, 1.0) & \hat{n}(1.0, 1.0) \\ \hat{n}(0.0, 0.5) & \hat{n}(0.5, 0.5) & \hat{n}(1.0, 0.5) \\ \hat{n}(0.0, 0.0) & \hat{n}(0.5, 0.0) & \hat{n}(1.0, 0.0) \end{bmatrix} \qquad (G2)$$

we wish to interpolate samples on the perimeter and interior of the plaquette.

First we consider the problem for the plaquette perimeter. Consider the points $\hat{n}(0.0, 0.0)$, $\hat{n}(1.0, 0.0)$, $\hat{n}(1.0, 1.0)$, $\hat{n}(0.0, 1.0)$ in counterclockwise order where for each segment, we need to interpolate between its endpoints. For example, we need to define $\hat{n}(0.5, 0.0)$ on the segment $\hat{n}(0.0, 0.0) \rightarrow \hat{n}(1.0, 0.0)$. Denote the initial and final points on the sphere in spin-space as $\hat{n}_i$ and $\hat{n}_f$. We use geodesics on the sphere consisting of great circles in order to describe a trajectory from $\hat{n}_i$ to $\hat{n}_f$ with minimal length. Explicitly, we take

$$\hat{n}(t) = \frac{\sin[\gamma(1-t)]}{\sin[\gamma]}\hat{n}_i + \frac{\sin[\gamma t]}{\sin[\gamma]}\hat{n}_f, \quad \cos(\gamma) = \vec{n}_i \cdot \vec{n}_f$$

$$(G3)$$

from which one can show $\hat{n}(t) \cdot \hat{n}(t) = 1$ ensuring $\hat{n}(t)$ lies on the sphere with $\cdot$ the dot product. In addition, $\hat{n}_i \cdot \hat{n}(t) = \cos[\gamma t]$ and $\hat{n}_f \cdot \hat{n}(t) = \cos[\gamma(1-t)]$ demonstrating the corresponding angles which measure distance on a sphere are linear in t.

Next we consider the plaquette interior. Consider again the points $\hat{n}(0.0, 0.0)$, $\hat{n}(1.0, 0.0)$, $\hat{n}(1.0, 1.0)$, $\hat{n}(0.0, 1.0)$ in counterclockwise order. By connecting each segment by geodesics as in Eq. G3, we trace out a region P bounded by a closed curve on the sphere with an interior defined by the right hand rule. One possible interpolation for the interior point $\hat{n}(0.5, 0.5)$ is the centroid of P. Since P lives on the sphere, the centroid of the complement P^C is also a sensible interpolation for $\hat{n}(0.5, 0.5)$. These two centroids $\vec{m}$, $\vec{m}^C$ are given by

$$\vec{m} = \frac{\int_P dA\,\hat{n}}{\int_P dA}, \quad \vec{m}^C = \frac{\int_{P^C} dA\,\hat{n}}{\int_{P^C} dA} = \frac{-\int_P dA\,\hat{n}}{4\pi - \int_P dA} \quad \text{(G4)}$$

where dA is the area element on the sphere and $\hat{n}$ is the normal on the sphere. We resolve this ambiguity by selecting the region with the smallest area from P and P^C. This gives the plaquette interior point as $\hat{n}(0.5, 0.5) = \vec{m}/|\vec{m}|$ if $\int_P dA \leq 2\pi$ and $\hat{S}(0.5, 0.5) = \vec{m}^C/|\vec{m}^C|$ otherwise.

The area integral in the dominator can be calculated explicitly for a region given by a spherical polygon consisting of M points $\hat{n}_0 \ldots \hat{n}_{M-1}$ connected by geodesics of the form in Eq. G3. It is given by

$$\int_P dA = \sum_{m=0}^{M-1} \theta_m - (M-2)\pi,$$

$$\tan(\theta_m) = \frac{\hat{n}_{m-1} \cdot (\hat{n}_m \times \hat{n}_{m+1})}{\hat{n}_{m-1} \cdot \hat{n}_{m+1} - (\hat{n}_{m-1} \cdot \hat{n}_m)(\hat{n}_{m+1} \cdot \hat{n}_m)} \quad \text{(G5)}$$

where θ_n is the interior angle defined by the three points $\hat{n}_{n-1}$, $\hat{n}_n$, $\hat{n}_{n+1}$, indices are taken modulo M, $\times$ denotes the cross product, and $\cdot$ denotes the dot product. The center of mass integral in the numerator can be calculated via Stokes theorem

$$\int_P dA\,\hat{n} = \frac{1}{2} \int dt\,\hat{n}(t) \times \frac{d\hat{n}(t)}{dt} =$$
$$\frac{1}{2} \sum_{m=0}^{M-1} \hat{n}_{m-1} \times \hat{n}_m \frac{\arccos(\hat{n}_{m-1} \cdot \hat{n}_m)}{\sqrt{1 - (\hat{n}_{m-1} \cdot \hat{n}_m)^2}} \quad \text{(G6)}$$

where $\hat{n}(t)$ parametrizes the geodesic defining the boundary of P and indices are taken modulo N.

[1] D. M. Stamper-Kurn, M. R. Andrews, A. P. Chikkatur, S. Inouye, H.-J. Miesner, J. Stenger, and W. Ketterle, Phys. Rev. Lett. **80**, 2027 (1998).

[2] J. M. Higbie, L. E. Sadler, S. Inouye, A. P. Chikkatur, S. R. Leslie, K. L. Moore, V. Savalli, and D. M. Stamper-Kurn, Phys. Rev. Lett. **95**, 050401 (2005).

[3] M. Vengalattore, S. R. Leslie, J. Guzman, and D. M. Stamper-Kurn, Phys. Rev. Lett. **100**, 170403 (pages 4) (2008).

[4] M. Vengalattore, J. Guzman, S. Leslie, F. Serwane, and D. M. Stamper-Kurn, *Crystalline magnetic order in a dipolar quantum fluid*, eprint arXiv:0901.3800 (2009).

[5] S. Giovanazzi, A. Görlitz, and T. Pfau, Phys. Rev. Lett. **89**, 130401 (2002).

[6] H. Pu, W. Zhang, and P. Meystre, Phys. Rev. Lett. **87**, 140405 (2001).

[7] S. Yi and H. Pu, Phys. Rev. Lett. **97**, 020401 (2006), ISSN 0031-9007.

[8] Y. Kawaguchi, H. Saito, and M. Ueda, Phys. Rev. Lett. **97**, 130404 (2006), ISSN 0031-9007.

[9] R. W. Cherng and E. Demler, Phys. Rev. Lett. **103**, 185301 (2009).

[10] Y. Kawaguchi, H. Saito, K. Kudo, and M. Ueda, *Magnetic crystallization of a ferromagnetic bose-einstein condensate*, eprint arXiv:0909.0565 (2009).

[11] J. Zhang and T.-L. Ho, *Spontaneous vortex lattices in quasi 2d dipolar spinor condensates*, eprint arXiv:0908.1593 (2009).

[12] R. W. Cherng and E. Demler, *Neutral skyrmion configurations in the low-energy effective theory of spinor condensate ferromagnets*, in preparation (2010).

[13] R. Rajaraman, *Solitons and Instantons* (North-Holland, Amsterdam, 1982).

[14] D. B. Litvin and W. Opechowski, Physica **76**, 538 (1974).

[15] C. J. Bradley and A. P. Cracknell, *The mathematical theory of symmetry in solids: representation theory for point groups and space gorups* (Clarendon, London, 1972).

[16] S. K. Kim, *Group Theoretical Methods and Applications to Molecules and Crystals* (Cambridge Univ. Press, Cambridge, 1999).

[17] D. B. Litvin, Acta Cryst. **A64**, 419 (2008).

[18] M. P. Allen and D. J. Tildesley, *Computer Simulation of Liquids* (Clarendon Press, Oxford, 1989).

[19] M. Artin, *Algebra* (Englewood Cliffs, NJ, 1991).

[20] F. Herbut, M. Vujicic, and Z. Papadopolos, J. Phys. A: Math. Gen. **13**, 2577 (1980).

[21] A. Zamorzaev, Sov. Phys-Cryst. **12**, 717 (1968).

[22] Here spin groups do not refer to the double cover of the orthogonal group that arises in the theory of Lie groups